Effect of Methane, CO 2 , and H 2 S on the Solubility of Methyl and Ethyl Mercaptans in a 25 wt % Methyldiethanolamine Aqueous Solution at 333 and 365 K

Christophe Coquelet, Eric Boonaert, Alain Valtz, Stanley Huang

Effect of methane, CO_2 and H_2S on the solubility of methyl and ethyl mercaptans in a 25wt% methyldiethanolamine aqueous solution at 333 and 365K

Christophe Coquelet[a,*], Eric Boonaert[a], Alain Valtz[a], Stanley Huang[b]

[a]*Mines ParisTech, PSL University, CTP-Centre of Thermodynamics of Processes, 35 rue Saint Honoré, 77305 Fontainebleau Cedex, France*

[b] *Former employee of Chevron, 1400 Smith Street, Houston, TX 77002*

*Corresponding author. Tel: +33164694962, E-mail address: christophe.coquelet@mines-paristech.fr (C. Coquelet)

Abstract

We have investigated the solubility of methanethiol and ethanethiol (methyl and ethyl mercaptans in an aqueous methyldiethanolamine solution (25 wt%) by using static-analytic method at 333 and 365K. The measurements were done for different pressure of methane in the absence of acid gas with individual acid gas present, and with mixture of acid gases present (CO_2 and/with H_2S). Additional measurement of Henry's law constant were realized by considering gas stripping method. Effect of total pressure (realized by addition of methane) and effect of acid gas loading for a constant total pressure around 7 MPa were studied. The increasing of pressure and acid gas loading increase the apparent Henry's law constant of the mercaptan, highlighting a drop out effect of the mercaptans.

Keywords:Data; Vapor–liquid equilibrium; Solubility, Henry's law constant, gas processing, experimental work

1. Introduction

Acid gases are present in natural gas and must be removed before its fractionation or liquefaction. Acid gas absorption[1] is the most popular operation unit considered to remove CO_2 and H_2S and this operation requires one solvent. Depending on the concentration of the acid gases, physical (pure organic compound in general) or chemical solvents are considered (Osman et al.[2]). In acid gas absorption, chemical solvent are generally preferred. They are aqueous alkanolamine solution where the chemical solvent reacts with CO_2 and H_2S to form regenerable salts. These salts are also thermally regenerable.

Unfortunately, H_2S is not the single sulfur compound presents in natural gas. If one of the hydrogen atoms of H_2S is replaced by an alkyl group, we have chemical from mercaptan or thiol family. methanethiol and ethanethiol are the two main sulfur compounds present in quantity with CO_2 and H_2S. According to Huguet et al.[3], the specification of typical treated gas contains minor amounts of contaminants: 2% CO_2, 2–4 ppm H_2S and 5–30 ppm total sulfur (mercaptans and COS). Mercaptans or thiols compounds are volatile compounds. They can be responsible of malodorous conditions and serious environmental concerns. Moreover, it is well known that mercaptans exhibit similar toxicity to hydrogen sulfide. In effect, very important quantity mercaptans may affect nervous system, can cause various health complications for example convulsion, narcosis, pulmonary oedema and so can paralyze respiratory system. As mercaptans are classified as acid component (R-SH) they can also cause serious corrosion problems and environmental damages due to acid deposition and rapid acidification. Some of them maybe introduced to the environment through anthropogenic resources not only fossil fuel burning or petrochemical industry but also from municipal sewage systems.

As mention by Awan et al.[4], environmental protection agencies force oil and gas companies reducing sulfur emission in effluent stream. Consequently, these restrictions led engineering companies to investigate the effects of these substances on the performances of amine systems (Pellegrini et al.[5] and Langè et al.[6],) particularly for acid gases removing using alkanolamine solvent.

It doesn't exist a large number of papers in the open literature concerning the solubility of methanethiol and ethanethiol in aqueous alkanolamine solution in the presence of acid gases. We can cite the work of Awan et al.[7] who studied the solubility of n-propylmercaptan in 50wt% MDEA aqueous solution. We can also cite the works of Coquelet and Richon[8], and Coquelet et al.[9] who have used gas stripping method to determine apparent Henry's law constant and limiting activity coefficient of mercaptans in different aqueous MDEA solutions. Jou and Mather[10] have published some solubility data of methanethiol (methyl mercaptan) in 50wt% aqueous MDEA solution at 40 and 70°C. In their paper, Jou and Mather have indicated that the presence of methanethiol doesn't affect the solubility of the acid gases. They have also investigated the measured data and analyzed the effect of methanethiol by comparing the variation Henry's law constant (calculated after computation of methanethiol fugacity) as a function of acid gas loading. It is important to notice that they have measured the methanethiol solubility at constant total pressure. They concluded that Henry's law constant is an increasing function with acid gas loading. This point was also highlighted by Bedell and Miller[1].

Why it is so important to consider the Henry's law constant? By definition the partition coefficient of component is defined by $K_i = \frac{C_i^g}{C_i^L}$ if we consider the molar concentrations in vapour and liquid phases. The molar concentration is defined by $C_i = \frac{n_i^{g\,or\,L}}{V^{g\,or\,L}}$ with n the mole number and V the volume of vapour or liquid phase. Moreover, at infinite dilution we can expressed the pressure by $P_i\varphi_i = \gamma_i^{\infty} x_i P_i^{sat}$ with φ_i the fugacity of component i, γ_i^{∞} the limiting activity coefficient of component i and P_i^{sat} the pure component vapour pressure of component i. At infinite dilution, φ_i is constant.

Considering the vapour phase we have $P_i = \frac{n_i^g ZRT}{Vg}$. Consequently, $K_i = \frac{C_i^g}{C_i^L} = \frac{y_i n^g V^L}{x_i n^L V g} = \frac{P_i V^L}{x_i n^L RTZ} = \frac{\gamma_i^{\infty} P_i^{sat} v^L}{ZRT\varphi_i}$ with v^L the molar volume of the solvent. The product $\frac{\gamma_i^{\infty} P_i^{sat}}{\varphi_i}$ is the apparent Henry's law constant and it is in effect the key thermodynamic we have to investigate.

In this paper, we have investigated the solubility of methanethiol and ethanethiol (methyl and ethyl mercaptan) in a 25wt% aqueous MDEA solution in the presence of CO_2, H_2S and CO_2 + H_2S. The objective of this work is to propose a methodology of work and to evaluate the effect of total pressure and acid gas loading on the liquid and vapor concentrations of mercaptans and there

apparent Henry's law constant. We have used two different techniques. The first one is the gas stripping method in order to determine the apparent Henry's law constant at infinite dilution and atmospheric pressure without methane, CO_2 and H_2S. The second one is based on static analytic method and is similar to the one used by Awan et al.[7].

2. Experimental part

2.1. Materials

In Table 1, the suppliers of of the different chemical species and their given purities are listed. Water (H_2O, CAS Number: 7732-18-5) was deionized and degassed.

Table 1: CAS Numbers, Purities and Suppliers of Materials.

Chemical Name	Formula	CAS No.	Purity mol%	Analysis method[a]	Supplier
Methyldiethanolamine (MDEA)	$C_5H_{15}NO_2$	105-59-9	>99	GC	Aldrich
Methanethiol (Methyl Mercaptan (MM))	CH_4S	74-93-1	>99	GC	Aldrich
Ethanethiol (Ethyl Mercaptan (EM))	C_2H_6S	75-08-1	>99	GC	Acros
Carbon dioxide	CO_2	124-38-9	99.995	GC	Air Liquide
Hydrogen sulfide	H_2S	7783-06-4	99.7	GC	Air Liquide
Methane	CH_4	74-82-8	99.995	GC	Messer
Water	H_2O	7732-18-5	Ultra pure (18.2 MΩ·cm)		Millipore/ Direct Q (direct-Q5)

[a] GC: Gas Chromatography

Table 2 presents the concentrations of the solvent loading with methanethiol and ethanethiol for the gas stripping measurement and the vapour liquid equilibrium measurement using static analytic-method. Solvents are prepared in a vessel by different weighing. First, the vessel is weighed under vacuum, than we add the MDEA, than the water and finally the mercaptan. Ethanethiol is added using a gas chromatograph syringe. Concerning methanethiol, as it is a gaseous component, we have connected the recipient directly to the MM bottle and controlled the quantity introduced by difference of pressure. The accuracy of the mass comparator used the different weighing (CC1200, METTLER TOLEDO) is ±1 mg. We have tried to prepare mixture with the same mercaptan global concentration close to 2000 ppm.

Table 2: Concentration of prepared 25 wt % MDEA aqueous solution for gas stripping and static-analytic measurements.

	gas stripping measurement		25 wt % MDEA aqueous solution								
			EM (2281ppm)			MM (2438ppm)			EM (1839ppm)		
	MDEA	H_2O	MDEA	H_2O	C_2H_5SH	MDEA	H_2O	CH_3SH	MDEA	H_2O	C_2H_5SH
M^a /g.mol^{-1}	119.61	18.02	119.16	18.02	62.14	119.16	18.02	48.11	119.16	18.02	48.11
m^b /g	300.12	100.02	81.39	243.94	2.0197	46.77	140.55	0.9632	79.59	238.81	1.5935
mass frac	0.7504	0.2496	0.2486	0.7452	0.0062	25.24	75.85	0.52	24.87	74.63	0.498
mol frac	0.048	0.952	0.04792	0.94980	2281 ppm	0.0478	0.9498	2438 ppm	0.0479	0.9503	1839 ppm
$U^c(x)$	6.10^{-7}	6.10^{-7}	6.10^{-7}	1.10^{-6}	1.10^{-6}	1.10^{-6}	3.10^{-6}	2.10^{-6}	6.10^{-7}	1.10^{-6}	1.10^{-6}

[a]: molar mass; [b]: mass of the component weighed. [C]: Expanded uncertainty on mole fraction (k=2)

2.2. Apparatus and method

a. Gas stripping measurement

The determination of the apparent Henry's Law Constant and Infinite Dilution Activity Coefficient are being measured using dilutor technique (gas stripping method). The measurements had been carried out from 25 till 75°C for the two mercaptans. 5 to 6 temperature points had been measured. The equipment is similar to the equipment used in previous work realized in our research group (Coquelet and Richon[8], Coquelet et al.[9], Zin et al.[11], Hajiw et al.[12]). Figure 1 shows the flowsheet of the experimental set-up employed to determine the apparent Henry's law constant. Briefly, two cells (saturator and dilutor cells) are immersed inside a liquid bath regulated to within 0.01 K. A platinum probe is inserted in the dilutor cell and is in immersed in the liquid phase. It is connected to an electronic display and is used for temperature readings. Considering supplier specification, the temperature uncertainty is estimated to be U(T) = 0.2 K. The exponential dilutor is not equipped with pressure transducer. In consequence, the value of atmospheric pressure is given by GE Druck DPI 142, Precision Barometic Indicator with an accuracy of U(P) = 0.04 kPa. Samples are analysed by a gas chromatograph (PERICHROM model PR2100, France) equipped with a flame ionization detector (FID) connected to a data software system. Helium is used as the carrier gas. The reference of the analytical column is 15% APIEZON L, 80/100 Mesh (Silcosteel, length 1.2 m, diameter 2 mm) from RESTEK, France. As presented in our previous papers, this method is based on the variation of vapor phase concentration when the highly diluted solute of the liquid mixture in the dilutor cell is stripped from the solution by a flow of inert gas (helium). Periodically, the concentration of the gas leaving the cell is sampled using a gas sampling valve

maintained at constant temperature. Samples are analyzed by gas chromatography. The peak area, S, of the solute decreases exponentially with the volume of inert gas flowing out from the cell.

In this experiment, 40 cm^3 of solvent (amine solution) is introduced into the "saturator cell", while about 50 cm^3 of the solvent is introduced into the "dilutor cell" (volume around 90cm^3) and few µg of solute is also added using a syringe. Thanks to a mass flow regulator, we can control the flow of the carrier gas. It bubbles through the stirred liquid phase and so permits the solute to be stripped into the vapor phase. It is important to note that equilibrium must be reached between the gas leaving the cell and the liquid phase in the cell. In order to check this point, we have to take attention that the measured activity coefficient value does not depend on the eluting gas flow-rate. The peak area of solute decreased exponentially with time if the analysis was made in the linearity range of the detector.

Equation 1 is considered to calculate the apparent Henry's Law coefficient, H_i (Pa), of solute *i*. Equation 1 is obtained considering mass balance around the equilibrium cell concerning the solute.

$$H_i = -\frac{1}{t}\ln\left(\frac{S_i}{(S_i)_{t=0}}\right).\ \frac{RTN}{\frac{D}{1-\frac{P^{sat}_{solv}}{P}}+\frac{V_G}{t}\ln\left(\frac{S_i}{(S_i)_{t=0}}\right)} \qquad (1)$$

where D is the carrier gas flow rate ($m^3.s^{-1}$); N is the total number of moles of solvent inside the dilutor cell; V_G (m^3) is the volume of the vapor phase inside the dilutor cell; S_i is the chromatograph solute *i* peak area; *t* (s) is the time; T (K) is the temperature inside the cell; P is the pressure inside the cell (around atmospheric pressure); P^{sat}_{solv} (Pa) is the saturation pressure of the solvent; and R ($J.mol^{-1}.K^{-1}$) is the ideal gas constant. Relative uncertainty concerning the Henry's law coefficient is estimated to be within 4.7 % (see Zin et al.[11] and Hajiw et al.[12] for more details).

This estimation comes from propagation of errors on the uncertainty of the solute *i* peak area determination, the uncertainties on the flow, the uncertainties related to the temperature and pressure, number of moles of solvent and accuracy of the approach (mass balance and hypothesis). Infinite Dilution Activity Coefficient,γ_i^{∞}, is calculated through equation (2):

$$\gamma_i^{\infty} = \frac{H_i P^{sat}_{solv}}{P^{sat}_i} \qquad (2)$$

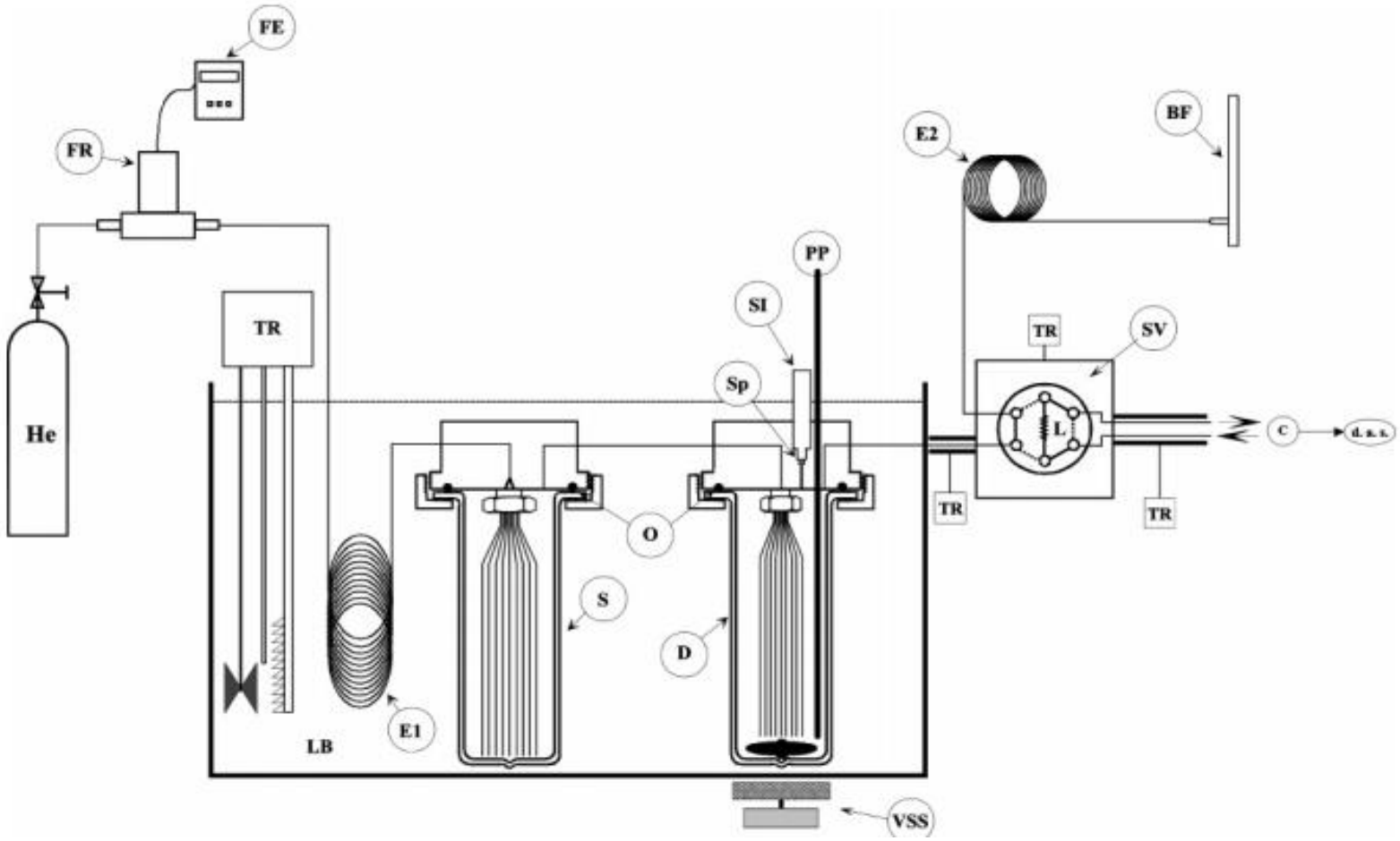

Figure 1: Flow diagram of the equipment: BF, bubble flow meter; C, gas chromatograph; D, dilutor; d.a.s., data acquisition system; He,helium cylinder; E1, E2, heat exchangers; FE, flow meter electronic; FR, flow regulator; L, sampling loop; LB, liquid bath; O, O-ring; PP,platinum resistance thermometer probe; S, saturator; SI, solute injector; Sp, septum; SV, sampling valve; TR, temperature regulator;VSS, variable speed stirrer.

The correlation (DIPPR n°101) to calculate saturation pressure is given in equation (3), with details concerning the calculation of the saturation pressure are presented Table 3.

$$P^{sat} = e^{\left(A+\frac{B}{T}+C\ln(T)+D\cdot T^{E}\right)} \quad (3)$$

Concerning the solvent, its vapor pressure is calculated using equation (4).

$$P^{sat}_{solv} = x_{water}P^{sat}_{water} + x_{MDEA}P^{sat}_{MDEA} \quad (4)$$

With x_i the mole fraction of component i. This equation is derived from $P = P_{water} + P_{MDEA} = \gamma_{water}x_{water}P^{sat}_{water} + \gamma_{MDEA}x_{MDEA}P^{sat}_{MDEA}$ with γ_i the activity coefficient of component i. Kim et al.[13] have shown with their measurements using ebulliometer that the activity coefficient is close to one for a 25wt% aqueous MDEA solution. Moreover, $P^{sat}_{MDEA} \ll P^{sat}_{water}$.

Table 3: Coefficient of the pure component vapor pressure correlation (Eq. 3).

Parameters	MM	EM	Water
A	54.15	65.551	73.649
B	-4337.7	-5027.4	-7258.2
C	-4.8127	-6.6853	-7.3037
D	$4.5\text{x}10^{-17}$	$6.32\text{x}10^{-6}$	$4.17\ \text{x}10^{-6}$
E	6	2	2

Source: Simulis™ thermodynamics from PROSIM, France.

b. Static analytic method

A "static-analytic" technique based on a closed-circuit method is used for the determination of partition coefficient methanethiol and ethanethiol in 50 wt% MDEA aqueous solution in the presence of CO_2 and H_2S. The equipment is similar to the one used by Dicko et al.[14], Awan et al.[7] and Skylogianni et al.[15]. The flowsheet of the equipment is presented in figure 2. Briefly, the apparatus is equipped with two online capillary samplers (ROLSI®, Armines' patent) connected to a gas chromatograph through a heated transfer line. The capillary samplers are capable of withdrawing micro samples without perturbing the equilibrium conditions over numerous samplings, thus leading to repeatable and reliable results. An internal stirring system with external motor reduced the time required to reach equilibrium. Analytical work was carried out using a gas chromatograph (PERICHROM model PR2100, France) equipped with a thermal conductivity

detector (TCD) and a flame ionization detector (FID) connected to a data software system. Helium is used as the carrier gas in this experiment. A Porapak R GC column is used (Porapak R 80 / 100 mesh, 2 m x 2 mm ID Silcosteel). Also a pre column used (length 0.25 m) in order to separate MDEA from the other species. Considering the value of the total pressure, we have considered that the mole ratio n_{water}/n_{MDEA} is constant.

The equilibrium cell temperature is measured at two points, one for vapor and the other for liquid phase by using two four-wire Pt100 Platinum Resistance Thermometer probes. Probes are inserted in the upper and lower flanges. The platinum probes are calibrated against a reference four-wire PT-25 Platinum Resistance Thermometer probe (PT-100). The 25 Ω reference platinum resistance thermometer (TINSLEY Precision Instruments) was calibrated by the Laboratoire National d'Essais (Paris) based on the 1990 International Temperature Scale (ITS 90). The resulting accuracy for temperature is not higher than ± 0.015 °C by the temperature range. The pressure transducers have been calibrated against a PACE 5000 Modular Pressure Calibrator (GE Sensing, France). Pressure measurement accuracy are estimated to be within ± 0.8 kPa. Calibration of GC detectors is realized by injection of known quantities of chemicals in the GC using GC syringe and eVol analytical electronic syringe. Several volumes of each component are injected in order to obtain a correlation to link mole number injected and the corresponding GC peak areas for the different GC detectors. Estimation of the detectors accuracy for each component are obtained with the help of polynomial expressions whereby the numbers of moles are expressed as a function of peak areas. Table 4 shows the results.

Table 4: Components and accuracy (typical accuracy values).

Component	Phase	Detector (sensitivity)	Mole number relative accuracy/ %
CH_4	Vapor	TCD (gain=0.5)	2.5
H_2O	Liquid	TCD (gain=0.5)	1.5
CO_2	Liquid/vapor	TCD (gain=0.5)	2.0
CH_4	Liquid	FID (10nA)	2.5
EM	Liquid	FID (10nA)	3.0
MM	Vapor	FID (10nA)	1.8
H_2S	Vapor	TCD (gain=0.05)	2.2
H_2S	Liquid	TCD (gain=0.5)	1.9

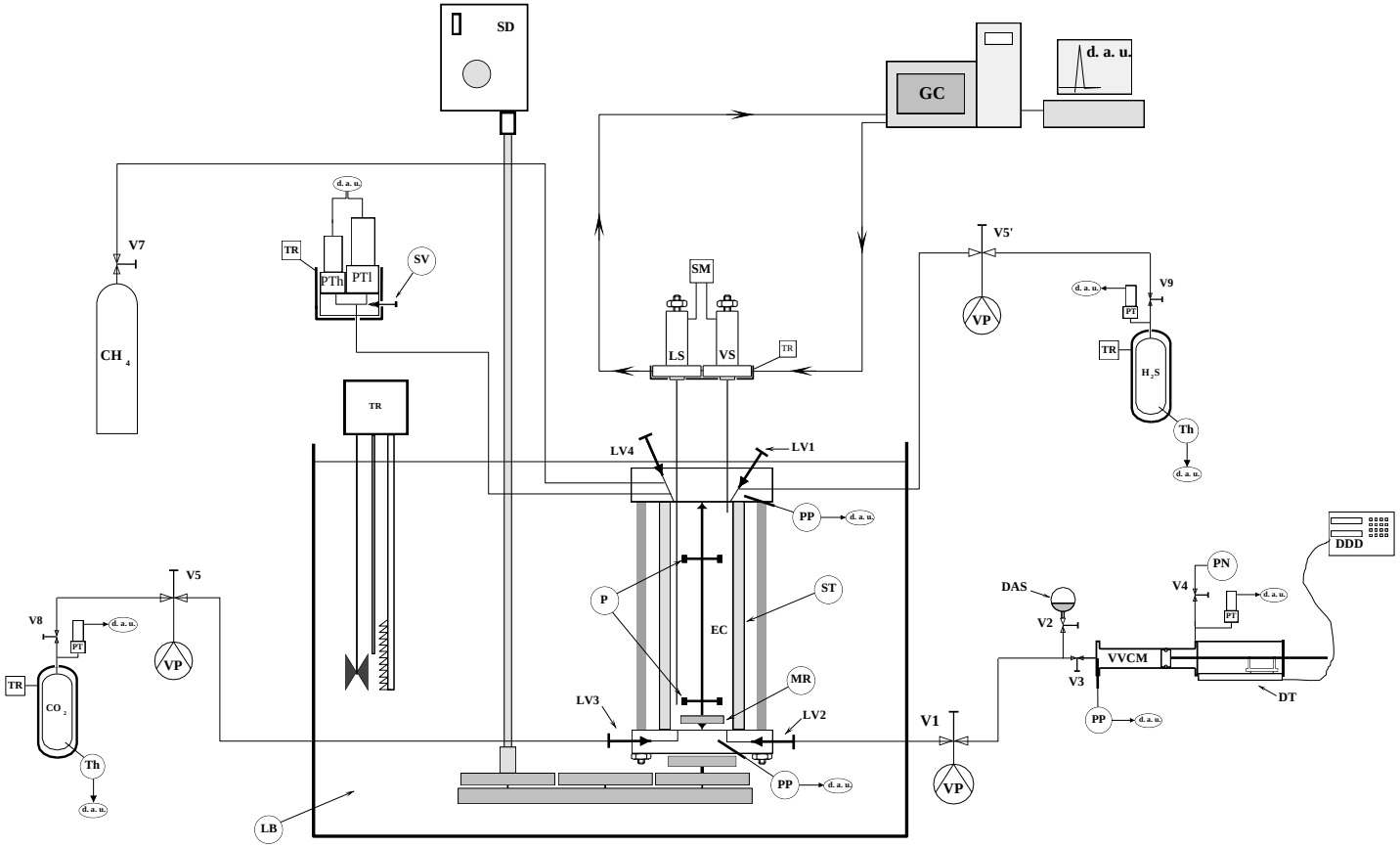

Figure 2: Schematic diagram of apparatus: DAS: Degassed Aqueous Solution; d. a. u. : Data Acquisition Unit ; DDD : Digital Displacement Display ; DM : Degassed Mixture ; DT : Displacement Transducer ; EC : Equilibrium Cell ; GC : Gas Chromatograph ; LB: Liquid Bath; LS : Liquid Sampler ; LVi : Loading Valve ; MR; Magnetic Rod; P: Propeller; PN: Pressurized nitrogen; PP : Platinum Probe ; PTh: Pressure transducer for high pressure values; PTl: Pressure transducer for low pressure values; PT: pressure transducer. SD : Stirring Device ; SM: Sample Monitoring; ST: Saphire tube; SV: Selection Valve; Th: Thermocouple; TR: Thermal Regulator; Vi: Valve; VP: Vacuum Pump; VS: Vapor Sampler; VVCM: Variable Volume Cell for Mixture

Measurement are done by fixing a total loading given by $L_{AG}^{total} = \frac{n_{AG}}{n_{MDEA}}$. n_{AG} is the total mole of acid gases introduced into the equilibrium cell. The calculation is done by considering information of T, P and volume of gas tank (separate reservoir). Densities at given T and P are calculated using REFPROP v10.0 software[16]. The loading of acid gases CO_2 or H_2S into the equilibrium cell is carried out through separate reservoirs having well known volumes (V). Each reservoir is filled with acid gas from the main gas cylinders. The pressure and temperature are continuously registered through data acquisition unit. Pressure inside the reservoirs are measured by means of two Druck™ pressure transducers (one for CO_2 and the other for H_2S) connected to the data acquisition unit (HP 34970A). The temperatures for the CO_2 press and the H_2S press are measured through two thermocouples which are also connected to the HP data acquisition unit. Total loading is calculated by considering the variation of T and difference of pressure during the loading (before and after the loading). Equation (5) presents the method of calculation.

$$L_i = \frac{n_i^{initial} - n_i^{final}}{n_{MDEA}} = V\frac{\rho_i(T^{initial},P^{initial}) - \rho_i(T^{final},P^{final})}{n_{MDEA}} \quad (5)$$

With ρ_i the density of the acid gas calculated using REFPROP v10.0. The most important loading is the exact loading calculated using GC analysis of liquid phase ($L_{AG}^{analysed} = \frac{x_{AG}}{x_{MDEA}}$). The exact loading should be lower than the total loading.

c. Uncertainty evaluation

The combined standard uncertainty of a quantity θ, u_c (θ) is obtained by equation (6).

$$u_c(\theta) = \pm\sqrt{u_{calib}(\theta)^2 + u_{rep}(\theta)^2} \quad (6)$$

with subscripts calib, rep denoting that of calibration, repeatability. The determination of the uncertainty of the concentration required the uncertainty of each mole numbers (see Table 4 for the different values of $u(n_i)/n_i$). The uncertainty of the mole fraction is determined after calibration of the GC detectors (Eqs. 7 and 8).

$$x_i = \frac{n_i}{\sum_i^{ncomp} n_i} \quad (7)$$

$$u(x_i) = \sqrt{\sum_{i}^{ncomp} \left(\frac{\partial x_i}{\partial n_i} \right)_{i \neq j}^{2} u^2(n_i)} \quad (8)$$

For example, for a binary system, one can calculate $u(x_1) = x_1(1-x_1)\sqrt{\left(\frac{u(n_1)}{n_1}\right)^2 + \left(\frac{u(n_2)}{n_2}\right)^2}$.

We consider for each mole number that we have uncertainty of Type B.

2.3. Experimental results

a. Gas stripping method

The results, apparent Henry's law constant and calculated limiting activity coefficient, are presented in Table 5 and plotted on figure 3.

Table 5: Temperature Dependence of Henry's Law Constant (H) and limiting activity coefficient (γ^{∞}) for methyl Mercaptan (MM) and ethyl Mercaptan (EM) in Water and in 25 wt % MDEA aqueous Solutions at atmospheric pressure[a].

MM			EM		
T/ K	**H/ MPa**	**γ^{∞}**	**T/ K**	**H/ MPa**	**γ^{∞}**
Water[a]			**Water[b]**		
298.6	16	78	298.4	25	354
308.6	22	80	308.3	33	329
323.5	33	77	318.4	48	338
333.4	42	75	323.3	54	322
348.3	60	74	333.3	73	320
			348.2	102	295
MDEA 25wt%[a]			**MDEA 25wt%[a]**		
298.4	2.1	10.4	298.5	4.1	58
308.3	2.6	9.4	308.2	5.7	57
318.3	3.5	9.2	318.3	9.1	64
323.3	4.5	10.6	323.3	10.6	64
333.3	6.9	12.3	333.3	15.5	68
348.2	9.2	11.4	348.2	24.8	72

[a] Expanded uncertainties (k=2) U(P)=0.04kPa, U(T)=0.2K, $U(H_i)/H_i$=4.7 %

[b] Results from Zin *et al.*[17]

Figure 3 illustrated the temperature dependence of the logarithm of the apparent Henry's law constant as a function of inverse temperature concerning the methanethiol and ethanethiol in pure water and in 25% wt% MDEA aqueous solution, respectively. As we can see, the apparent Henry's law constant is lower in the alkanolamine solution as the solubility of mercaptan is higher in 25wt% aqueous MDEA solution. Also we can see that the apparent henry's law constant of methanethiol is lower than the one for ethanethiol. It is due to the presence of supplementary carbon atom in the ethanethiol. We can also notice that the trend between the logarithms of the apparent Henry's law constant versus the inverse of temperature is linear. It signifies that the heat of absorption, associated to the slope of the linear curve, is not strongly temperature dependent.

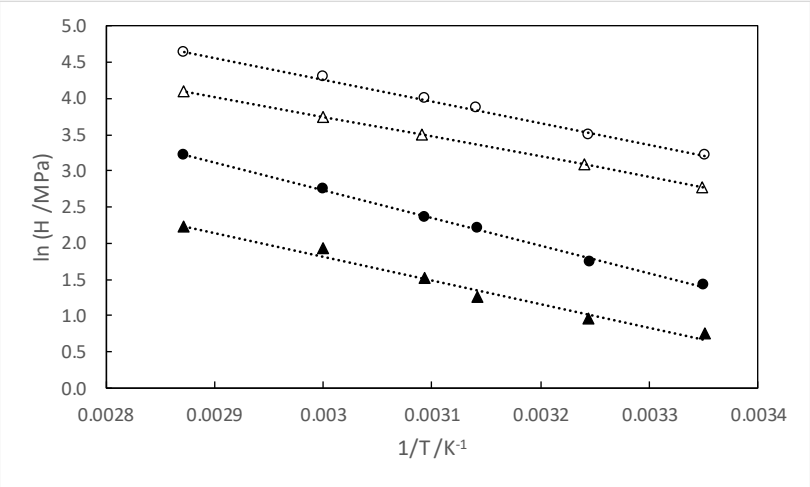

Figure 3: Logarithm of apparent Henry's law constant of methanethiol (Δ) and ethanethiol (o) in water and in MDEA weight fractions of 25 % as a function of inverse temperature. (empty symbol: water, bold symbols 25 wt% MDEA).

b. Static analytic method

The list of experimental data point realized is presented in Table 6. The results without acid gases for MM and EM are presented in Tables 7 and 8 respectively. Results with CO_2 for MM and EM are presented in Tables 9 to 12. Results with H_2S for MM and EM are presented in Tables 13 to 16. Results with CO_2 and H_2S for MM and EM are presented in Tables 17 to 22. Each table of results is divided into two parts. In the first part, mole fraction of each component in each phase, the number of sample, the standard deviation ($\sigma = \sqrt{\frac{1}{n-1}\sum_1^N \left(x_i - \frac{\sum_1^N x_i}{n}\right)^2}$) and acid gases loading

are presented. In the second part, the corresponding calibration uncertainties for each component are presented. Using our experimental results we have calculated the apparent Henry's law constant. It is defined by equation (10). K_i is the partition coefficient.

Table 6: List of experimental VLE data realized. Pressurization will be done using CH_4.

System	T / K	P / MPa	No. of Experimental data
MM + CO_2 (no H_2S)	333 and 365	Around 7	6 (3 pts /T)
MM + H_2S (no CO_2)	333 and 365	Around 7	6
MM + H_2S (3 CO_2 loadings)	333 and 365	Around 7	6
EM + H_2S (no CO_2)	333 and 365	Around 7	6
EM + CO_2 (no H_2S)	333 and 365	Around 7	6
EM + CO_2 (3 H_2S loadings)	333 and 365	Around 7	6

$$H_i = \frac{Py_i}{x_i} = PK_i \qquad (10)$$

Using our experimental results, we have compared the influence of mercaptan concentration, total pressure and acid gases loading on the variation of the apparent Henry's law constant. We have considered the apparent Henry's law constant measured by gas stripping method as the reference. The table 7 presents the results concerning the two mercaptans without any acid gases. The results are also plotted in figure 4. We can observed a linear dependency between apparent Henry's law constant and total pressure and a continuity from measurement using gas stripping method for EM but not for MM. We can suspect that it may be due to the fact chemical reaction between MM and aqueous MDEA solution is more important than with EM (certainly, there is no chemical reaction with EM). Methane, which is not present during gas stripping measurement, may inhibit the reaction with MM and drop out MM for the solution. Another explanation can be that the rate of the reaction is very low in comparison to the residence time of the MM in comparison to the time of stripping. Probably it leads to some inaccuracy with gas stripping measurement method. In Tables 23 to 26 apparent Henry's law constant are calculated.

On each table of results, we did not include the vapor concentration of water. A rough estimation can be done by divided the water vapor pressure by the total pressure. At 333K and 7MPa, the water concentration is approximatively equal to 0.003 mole/mole, and at 365K and 7 MPa, the

value is close to 0.1 mole/mole. During our experiments, using our experimental technique we did not observe any presence of water in the vapor phase. This can be due to the fact that its concentration is too low and it is lower than the limit of detection of our analytical device (Gas Chromatograph). Also, it signifies that the value of the water concentration in the vapor phase is lower than the previous estimated values (estimated values using water vapor pressure correspond to the maximum value of water concentration in vapor phase). Our experiments are realized in the presence of methane. It is well known that the water content in vapor phase is a decreasing function of methane pressure. In the GPSA handbook[18] several correlations are proposed and the correlations predict that the water content decreases when the pressure increases. Also, in their papers on the estimation of the water vapor content of the $CH_4 - H_2O$ binary system, Chapoy et al.[19, 20] show also that the water content decreases with an increasing of the pressure. For example, at 313.12 K and 6.056 MPa, the water content is 0.001516 mole/mole and at 318.12 K and 6.017 MPa the water content is 0.001985 mole/mole. Consequently, considering our system with several chemical species, the water content would be very low and not detectable using our analytical device.

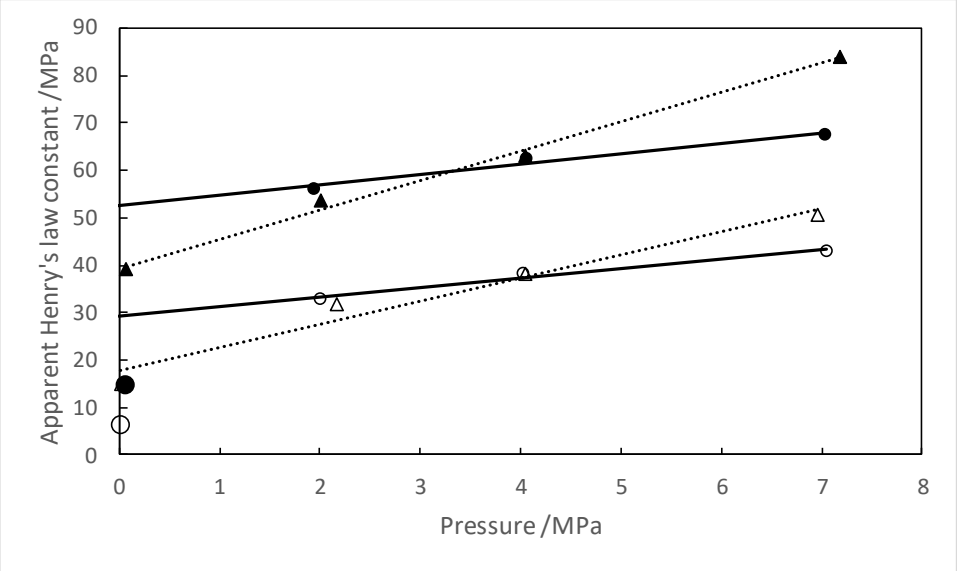

Figure 4: Variation for Methanethiol (o) and Ethanethiol (Δ) apparent Henry's law constant as a function of total pressure. Empty symbol: 333K, black symbol: 365 K. Lines: linear tendency curve.

Table 7: Vapor Liquid equilibrium data of Methanethiol (2438 ppm) in 25 wt% MDEA aqueous solution. δx corresponds to the standard deviation due to repeatability measurements and u(x) corresponds to uncertainties due to GC detectors calibration

T^a	P^a		MM		CH_4		MDEA		H_2O^b			MM		CH_4	
K	MPa	n	x	δx	x	δx	x	δx	x	δx	n	y	δy	y	δy
332.68	2.0033	6	0.00253	2E-05	0.00041	2E-06	0.04777	9E-07	0.94929	2E-05	4	0.04123	1E-04	0.95877	1E-04
332.71	4.0292	6	0.00210	2E-05	0.00084	2E-05	0.04777	2E-06	0.94929	4E-05	5	0.01987	1E-05	0.98013	1E-05
332.69	7.0543	7	0.00167	3E-05	0.00145	1E-05	0.04776	1E-06	0.94912	2E-05	6	0.01013	3E-05	0.98987	3E-05
364.54	1.9405	7	0.00205	3E-05	0.00039	5E-06	0.04780	2E-06	0.94977	4E-05	10	0.05917	9E-05	0.94083	9E-05
364.58	4.0580	7	0.00178	2E-05	0.00087	1E-05	0.04779	1E-06	0.94957	3E-05	4	0.02742	1E-05	0.97258	1E-05
364.60	7.0408	7	0.00157	2E-05	0.00153	1E-05	0.04776	1E-06	0.94914	3E-05	5	0.01503	2E-05	0.98497	2E-05

T	MM	CH_4	MM	CH_4	MDEA	H_2O	T	MM	CH_4	MM	CH_4	MDEA	H_2O
K	u(y)	u(y)	u(x)	u(x)	u(x)	u(x)	K	u(y)	u(y)	u(x)	u(x)	u(x)	u(x)
332.68	1E-04	2E-03	5E-05	7E-06	1E-03	2E-02	364.54	2E-04	2E-03	4E-05	7E-06	1E-03	2E-02
332.71	6E-05	2E-03	4E-05	2E-05	1E-03	2E-02	364.58	8E-05	2E-03	4E-05	2E-05	1E-03	2E-02
332.69	3E-05	2E-03	3E-05	3E-05	1E-03	2E-02	364.60	4E-05	2E-03	3E-05	3E-05	1E-03	2E-02

[a] Expanded uncertainties (k=2) U(P)=0.0008MPa, U(T)=0.02K [b]Vapor water content is not measured and lower than the limit of detection of the TCD detector

Table 8: Vapor Liquid equilibrium measurements with Ethanethiol (2281 ppm) in 25 wt% MDEA aqueous solution at 333 and 363 K. δx corresponds to the standard deviation due to repeatability measurements and u(x) corresponds to uncertainties due to GC detectors calibration.

T[a]	P[a]		EM		CH_4		MDEA		H_2O[b]			EM		CH_4	
K	MPa	n	x	δx	x	δx	x	δx	x	δx	n	y	δy	y	δy
333.30	2.1754	9	0.000539	3E-06	0.000378	2E-06	0.0479860	2E-07	0.951097	4E-06	6	0.00789	2E-05	0.99211	2E-05
333.32	4.0419	7	0.000496	6E-06	0.000692	4E-06	0.0479729	4E-07	0.950839	8E-06	6	0.004665	5E-06	0.995335	5E-06
333.28	6.9601	14	0.000410	3E-06	0.001130	7E-06	0.0479560	4E-07	0.950504	7E-06	8	0.00297	3E-05	0.99703	3E-05
365.12	2.0088	9	0.000509	3E-06	0.00037	1E-05	0.0479876	6E-07	0.95113	1E-05	5	0.01360	3E-05	0.98640	3E-05
365.12	4.0410	6	0.000451	5E-06	0.00078	2E-05	0.0479709	9E-07	0.95080	2E-05	8	0.00704	6E-05	0.99296	6E-05
365.12	7.1768	7	0.000350	4E-06	0.001269	8E-06	0.0479522	3E-07	0.950428	6E-06	6	0.00410	2E-05	0.99590	2E-05

T	EM	CH_4	MM	CH_4	MDEA	H_2O	T	EM	CH_4	MM	CH_4	MDEA	H_2O
K	u(y)	u(y)	u(x)	u(x)	u(x)	u(x)	K	u(y)	u(y)	u(x)	u(x)	u(x)	u(x)
333.30	6E-05	5E-03	2E-05	7E-06	8E-04	2E-02	365.12	1E-04	5E-03	2E-05	7E-06	8E-04	2E-02
333.32	3E-05	5E-03	2E-05	1E-05	8E-04	2E-02	365.12	5E-05	5E-03	2E-05	1E-05	8E-04	2E-02
333.28	2E-05	5E-03	2E-05	2E-05	8E-04	2E-02	365.12	3E-05	5E-03	1E-05	2E-05	8E-04	2E-02

[a] Expanded uncertainties (k=2) U(P)=0.0008MPa, U(T)=0.02K [b]Vapor water content is not measured and lower than the limit of detection of the TCD detector

Table 9: Vapor Liquid equilibrium data of Methanethiol (2438 ppm) in 25 wt% MDEA aqueous solution with CO_2 (total loading 0.257 and 0.486). δx corresponds to the standard deviation due to repeatability measurements and u(x) corresponds to uncertainties due to GC detectors calibration.

T[a]	P[a]		MM		CH_4		CO_2		MDEA		H_2O[b]		CO_2 Loading
K	MPa	n	x	δx	x	δx	x	δx	x	δx	x	δx	
332.70	7.0019	7	0.00176	1E-05	0.00111	4E-06	0.01084	9E-05	0.047256	5E-06	0.93904	9E-05	0.229
332.69	6.9884	7	0.00132	1E-05	9.35E-04	1E-06	0.02247	1E-04	0.046728	6E-06	0.92855	1E-04	0.481

T[a]	P[a]		MM		CH_4		CO_2	
K	MPa	n	y	δy	y	δy	y	δy
332.70	7.0019	7	0.01773	4E-05	0.98143	5E-05	0.00084	1E-05
332.69	6.9884	7	0.01596	1E-04	0.97736	9E-05	0.00668	6E-05

T	MM	CH_4	CO_2	MM	CH_4	CO_2	MDEA	H_2O
K	u(y)	u(y)	u(y)	u(x)	u(x)	u(x)	u(x)	u(x)
332.70	5E-05	2E-03	1E-05	4E-05	2E-05	2E-04	9E-04	2E-02
332.69	5E-05	2E-03	7E-05	3E-05	2E-05	5E-04	9E-04	2E-02

[a] Expanded uncertainties (k=2) U(P)=0.0008MPa, U(T)=0.02K [b]Vapor water content is not measured and lower than the limit of detection of the TCD detector

Table 10: Vapor Liquid equilibrium data of Methanethiol (2438 ppm) in 25 wt% MDEA aqueous solution with CO_2 (total loading 0.257 and 0.486). δx corresponds to the standard deviation due to repeatability measurements and u(x) corresponds to uncertainties due to GC detectors calibration.

T^a	P^a		MM		CH_4		CO_2		MDEA		H_2O^b		CO_2 Loading
K	MPa	n	x	δx	x	δx	x	δx	x	δx	x	δx	
364.60	7.0092	6	0.00146	2E-05	1.16E-03	6E-06	0.00887	9E-05	0.047362	5E-06	0.94115	1E-04	0.187
364.60	7.0108	8	0.00136	2E-05	1.03E-03	1E-05	0.01936	3E-04	0.046870	2E-05	0.93137	3E-04	0.413

T^a	P^a		MM		CH_4		CO_2	
K	MPa	n	y	δy	y	δy	y	δy
364.60	7.0092	5	0.02131	8E-05	0.97190	9E-05	0.00679	5E-05
364.60	7.0108	6	0.02111	8E-05	0.95021	1E-04	0.02868	1E-04

T	MM	CH_4	CO_2	MM	CH_4	CO_2	MDEA	H_2O
K	u(y)	u(y)	u(y)	u(x)	u(x)	u(x)	u(x)	u(x)
364.60	6E-05	2E-03	8E-05	3E-05	2E-05	2E-04	9E-04	2E-02
364.60	6E-05	2E-03	3E-04	3E-05	2E-05	4E-04	9E-04	2E-02

[a] Expanded uncertainties (k=2) U(P)=0.0008MPa, U(T)=0.02K [b]Vapor water content is not measured and lower than the limit of detection of the TCD detector

Table 11: Vapor Liquid equilibrium measurements with Ethanethiol (2281 ppm) in 25 wt% MDEA aqueous solution with CO_2. (total loading 0.188 and 0.445). δx corresponds to the standard deviation due to repeatability measurements and u(x) corresponds to uncertainties due to GC detectors calibration.

T^a	P^a		EM		CH_4		CO_2		MDEA		H_2O^b		CO_2 Loading
K	MPa	n	x	δx	x	δx	x	δx	x	δx	x	δx	
333.35	7.0080	14	0.00030	5E-06	0.001038	5E-06	0.0074	8E-05	0.0476	4E-06	0.944	7E-05	0.155
333.35	7.0350	13	0.00027	3E-06	0.00091	5E-06	0.0146	5E-05	0.0472	3E-06	0.937	5E-05	0.309

T^a	P^a		EM		CH_4		CO_2	
K	MPa	n	y	δy	y	δy	y	δy
333.35	7.0080	5	0.00388	3E-05	0.995	3E-05	0.00131	8E-06
333.35	7.0350	5	0.00419	5E-05	0.991	1E-04	0.00429	6E-05

T	CH_4	CO_2	H_2O	MDEA	EM	CH_4	CO_2	EM
K	u(x)	u(x)	u(x)	u(x)	u(x)	u(y)	u(y)	u(y)
333.35	2E-05	2E-04	2E-02	8E-04	1E-05	5E-03	2E-05	3E-05
333.35	2E-05	3E-04	2E-02	8E-04	1E-05	5E-03	6E-05	3E-05

[a] Expanded uncertainties (k=2) U(P)=0.0008MPa, U(T)=0.02K [b]Vapor water content is not measured and lower than the limit of detection of the TCD detector

Table 12: Vapor Liquid equilibrium measurements with Ethanethiol (2281 ppm) in 25 wt% MDEA aqueous solution with CO_2. (total loading 0.188 and 0.445). δx corresponds to the standard deviation due to repeatability measurements and u(x) corresponds to uncertainties due to GC detectors calibration.

T^a	P^a		EM		CH_4		CO_2		MDEA		H_2O^b		CO_2 Loading
K	MPa	n	x	δx	x	δx	x	δx	x	δx	x	δx	
365.12	7.0056	6	0.00026	4E-06	0.00110	1E-05	0.00668	4E-05	0.0476	2E-06	0.944	5E-05	0.140
365.12	6.9841	7	0.00025	2E-06	0.00097	3E-06	0.01199	3E-05	0.0474	1E-06	0.939	3E-05	0.253

T^a	P^a		EM		CH_4		CO_2	
K	MPa	n	y	δy	y	δy	y	δy
365.12	7.0056	5	0.00448	3E-05	0.989	5E-05	0.00614	3E-05
365.12	6.9841	8	0.00489	3E-05	0.978	9E-05	0.01733	1E-04

T	CH_4	CO_2	H_2O	MDEA	EM	CH_4	CO_2	EM
K	u(x)	u(x)	u(x)	u(x)	u(x)	u(y)	u(y)	u(y)
365.12	2E-05	1E-04	2E-02	8E-04	1E-05	5E-03	8E-05	3E-05
365.12	2E-05	3E-04	2E-02	8E-04	1E-05	5E-03	2E-04	3E-05

[a] Expanded uncertainties (k=2) U(P)=0.0008MPa, U(T)=0.02K [b]Vapor water content is not measured and lower than the limit of detection of the TCD detector

Table 13: Vapor Liquid equilibrium data of Methanethiol (2438 ppm) in 25 wt% MDEA aqueous solution with H_2S (total loading 0.214 and 0.402). δx corresponds to the standard deviation due to repeatability measurements and u(x) corresponds to uncertainties due to GC detectors calibration.

T[a]	P[a]		MM		CH_4		H_2S		MDEA		H_2O[b]		H_2S Loading
K	MPa	n	x	δx	x	δx	x	δx	x	δx	x	δx	
333.34	7.0027	5	0.00197	1E-05	0.00122	1E-05	0.00975	4E-05	0.0472924	2E-06	0.93976	4E-05	0.206
332.72	6.9818	9	0.00197	6E-06	0.00111	5E-06	0.01730	9E-05	0.04694	4E-06	0.93269	9E-05	0.368

T[a]	P[a]		MM		CH_4		H_2S	
K	MPa	n	y	δy	y	δy	y	δy
333.34	7.0027	6	0.01724	6E-05	0.98110	7E-05	0.00165	1e-05
332.72	6.9818	6	0.01781	2E-04	0.97823	2E-04	0.00395	3E-05

T	MM	CH_4	H_2S	MM	CH_4	H_2S	MDEA	H_2O
K	u(y)	u(y)	u(y)	u(x)	u(x)	u(x)	u(x)	u(x)
333.34	5E-05	2E-03	2E-05	5E-05	2E-05	2E-04	9E-04	2E-02
332.72	5E-05	2E-03	4E-05	5E-05	2E-05	4E-04	9E-04	2E-02

[a] Expanded uncertainties (k=2) U(P)=0.0008MPa, U(T)=0.02K [b]Vapor water content is not measured and lower than the limit of detection of the TCD detector

Table 14: Vapor Liquid equilibrium data of Methanethiol in 25 wt% MDEA aqueous solution with H_2S (total loading 0.214 and 0.402). δx corresponds to the standard deviation due to repeatability measurements and u(x) corresponds to uncertainties due to GC detectors calibration.

T^a	P^a		MM		CH_4		H_2S		MDEA		H_2O^b		H_2S Loading
K	MPa	n	x	δx	x	δx	x	δx	x	δx	x	δx	
364.61	7.0790	6	0.00181	2E-05	0.00126	4E-06	0.00907	7E-05	0.047331	3E-06	0.94052	6E-05	0.192
364.59	6.9732	9	0.00171	5E-06	0.00115	6E-06	0.01618	6E-05	0.047001	3E-06	0.93397	6E-05	0.344

T^a	P^a		MM		CH_4		H_2S	
K	MPa	n	y	δy	y	δy	y	δy
364.61	7.0790	6	0.02120	5E-05	0.97460	4E-05	0.00420	3E-05
364.59	6.9732	6	0.02317	4E-05	0.96630	4E-05	0.01053	4E-05

T	MM	CH_4	H_2S	MM	CH_4	H_2S	MDEA	H_2O
K	u(y)	u(y)	u(y)	u(x)	u(x)	u(x)	u(x)	u(x)
364.61	6E-05	2E-03	4E-05	4E-05	3E-05	2E-04	9E-04	2E-02
364.59	7E-05	2E-03	1E-04	4E-05	2E-05	4E-04	9E-04	2E-02

[a] Expanded uncertainties (k=2) U(P)=0.0008MPa, U(T)=0.02K [b]Vapor water content is not measured and lower than the limit of detection of the TCD detector

Table 15: Vapor Liquid equilibrium measurements with Ethanethiol (2281ppm) in 25 wt% MDEA aqueous solution H_2S (total loading 0.215 and 0.419). δx corresponds to the standard deviation due to repeatability measurements and u(x) corresponds to uncertainties due to GC detectors calibration.

T[a]	P[a]		EM		CH_4		H_2S		MDEA		H_2O[b]		H_2S Loading
K	MPa	n	x	δx	x	δx	x	δx	x	δx	x	δx	
333.37	6.9843	6	0.00041	5E-06	0.00109	1E-05	0.0063	1E-04	0.0476	5E-06	0.944	9E-05	0.132
333.29	6.9840	11	0.00037	4E-06	0.00095	9E-06	0.0151	4E-04	0.0472	2E-05	0.936	3E-04	0.320

T[a]	P[a]		EM		CH_4		H_2S	
K	MPa	n	y	δy	y	δy	y	δy
333.37	6.9843	5	0.00409	2E-05	0.995	2E-05	0.00078	1E-05
333.29	6.9840	6	0.00410	5E-05	0.993	6E-05	0.00303	5E-05

T	CH_4	H_2S	H_2O	MDEA	EM	CH_4	H_2S	EM
K	u(x)	u(x)	u(x)	u(x)	u(x)	u(y)	u(y)	u(y)
333.37	2E-05	2E-04	9E-05	8E-04	2E-05	5E-03	2E-05	3E-05
333.29	2E-05	4E-04	3E-04	8E-04	1E-05	5E-03	6E-05	3E-05

[a] Expanded uncertainties (k=2) U(P)=0.0008MPa, U(T)=0.02K [b]Vapor water content is not measured and lower than the limit of detection of the TCD detector

Table 16: Vapor Liquid equilibrium measurements with Ethanethiol (2281 ppm) in 25 wt% MDEA aqueous solution H_2S (total loading 0.215 and 0.419). δx corresponds to the standard deviation due to repeatability measurements and u(x) corresponds to uncertainties due to GC detectors calibration.

T[a]	P[a]		EM		CH_4		H_2S		MDEA		H_2O[b]		H_2S Loading
K	MPa	n	x	δx	x	δx	x	δx	x	δx	x	δx	
365.13	7.0083	5	0.00035	5E-06	0.00108	3E-05	0.0048	7E-05	0.0477	2E-06	0.946	4E-05	0.101
365.13	6.9835	12	0.00034	5E-06	0.00098	1E-05	0.0145	2E-04	0.0472	1E-05	0.937	2E-04	0.307

T[a]	P[a]		EM		CH_4		H_2S	
K	MPa	n	y	δy	y	δy	y	δy
365.13	7.0083	5	0.00467	1E-05	0.993	3E-05	0.00224	2E-05
365.13	6.9835	7	0.00516	5E-05	0.986	9E-05	0.00866	1E-04

T	CH_4	H_2S	H_2O	MDEA	EM	CH_4	H_2S	EM
K	u(x)	u(x)	u(x)	u(x)	u(x)	u(y)	u(y)	u(y)
365.13	2E-05	1E-04	2E-02	8E-04	1E-05	5E-03	4E-05	3E-05
365.13	2E-05	4E-04	2E-02	8E-04	1E-05	5E-03	2E-04	4E-05

[a] Expanded uncertainties (k=2) U(P)=0.0008MPa, U(T)=0.02K [b]Vapor water content is not measured and lower than the limit of detection of the TCD detector

Table 17: Partition coefficient of Methanethiol (2438 ppm) in 25 wt% MDEA aqueous solution with CO_2 and H_2S (respective total loadings 0.232 and 0.206). δx corresponds to the standard deviation due to repeatability measurements and u(x) corresponds to uncertainties due to GC detectors calibration.

T[a]	P[a]		MM		CH_4		CO_2		H_2S		MDEA		H_2O[b]		Loadings	
K	MPa	n	x	δx	x	δx	x	δx	x	δx	x	δx	x	δx	CO_2	H_2S
332.66	6.9954	7	0.00268	2E-05	0.00118	4E-06	0.01177	6E-05	0.01046	5E-05	0.046662	3E-06	0.92724	7E-05	0.252	0.224
364.59	6.9599	8	0.00241	2E-05	0.00122	2E-06	0.00979	9E-05	0.00992	8E-05	0.046795	8E-06	0.92987	2E-04	0.209	0.212

T[a]	P[a]		MM		CH_4		CO_2		H_2S	
K	MPa	n	y	δy	y	δy	y	δy	y	δy
332.66	6.9954	5	0.02339	2E-05	0.97219	5E-05	0.00228	4E-05	0.00214	1E-05
364.59	6.9599	6	0.03106	9E-06	0.94874	7E-05	0.01407	4E-05	0.00613	7E-05

T	MM	CH_4	CO_2	H_2S	MM	CH_4	CO_2	H_2S	MDEA	H_2O
K	u(y)	u(y)	u(y)	u(y)	u(x)	u(x)	u(x)	u(x)	u(x)	u(x)
332.66	7E-05	2E-03	3E-05	2E-05	6E-05	2E-05	3E-04	2E-04	7E-05	2E-03
364.59	9E-05	2E-03	2E-04	6E-05	5E-05	2E-05	2E-04	2E-04	9E-05	2E-03

[a] Expanded uncertainties (k=2) U(P)=0.0008MPa, U(T)=0.02K [b]Vapor water content is not measured and lower than the limit of detection of the TCD detector

Table 18: Partition coefficient of Methanethiol (2438 ppm) in 25 wt% MDEA aqueous solution with CO_2 and H_2S (respective total loadings 0.429 and 0.224). δx corresponds to the standard deviation due to repeatability measurements and u(x) corresponds to uncertainties due to GC detectors calibration.

T[a]	P[a]		MM		CH_4		CO_2		H_2S		MDEA		H_2O[b]		Loadings	
K	MPa	n	x	δx	x	δx	x	δx	x	δx	x	δx	x	δx	CO_2	H_2S
332.67	6.9824	6	0.00216	2E-05	0.00107	1E-05	0.01981	1E-04	0.01086	1E-04	0.04629	1E-05	0.91980	2E-04	0.428	0.235
364.52	7.0457	18	0.00173	1E-05	0.00104	6E-06	0.01401	1E-04	0.00929	1E-04	0.04666	1E-05	0.92726	2E-04	0.300	0.199

T[a]	P[a]		MM		CH_4		CO_2		H_2S	
K	MPa	n	y	δy	y	δy	y	δy	y	δy
332.67	6.9824	5	0.01662	3E-05	0.97337	8E-05	0.00652	3E-05	0.00350	6E-05
364.52	7.0457	7	0.02276	7E-05	0.94292	3E-04	0.02617	1E-04	0.00815	1E-04

T	MM	CH_4	CO_2	H_2S	MM	CH_4	CO_2	H_2S	MDEA	H_2O
K	u(y)	u(y)	u(y)	u(y)	u(x)	u(x)	u(x)	u(x)	u(x)	u(x)
332.67	5E-05	2E-03	7E-05	4E-05	5E-05	2E-05	4E-04	2E-04	5E-05	2E-03
364.52	6E-05	2E-03	3E-04	8E-05	4E-05	2E-05	3E-04	2E-04	6E-05	2E-03

[a] Expanded uncertainties (k=2) U(P)=0.0008MPa, U(T)=0.02K [b]Vapor water content is not measured and lower than the limit of detection of the TCD detector

Table 19: Partition coefficient of Methanethiol (2438 ppm) in 25 wt% MDEA aqueous solution with CO_2 and H_2S (respective total loadings 0.231 and 0.413). δx corresponds to the standard deviation due to repeatability measurements and u(x) corresponds to uncertainties due to GC detectors calibration.

T[a]	P[a]		MM		CH_4		CO_2		H_2S		MDEA		H_2O[b]		Loadings	
K	MPa	n	x	δx	x	δx	x	δx	x	δx	x	δx	x	δx	CO_2	H_2S
332.65	6.9249	7	0.00215	3E-05	0.00106	2E-05	0.00911	2E-04	0.02074	3E-04	0.04633	2E-05	0.92062	4E-04	0.197	0.448
364.56	6.6968	7	0.00174	1E-05	0.00099	1E-05	0.00766	4E-05	0.01838	2E-04	0.04653	1E-05	0.92469	2E-04	0.165	0.395

T[a]	P[a]		MM		CH_4		CO_2		H_2S	
K	MPa	n	y	δy	y	δy	y	δy	y	δy
332.65	6.9249	6	0.01551	4E-05	0.97232	9E-05	0.00543	7E-05	0.00674	1E-04
364.56	6.6968	8	0.01972	1E-04	0.94319	2E-04	0.01996	2E-04	0.01713	2E-04

T	MM	CH_4	CO_2	H_2S	MM	CH_4	CO_2	H_2S	MDEA	H_2O
K	u(y)	u(y)	u(y)	u(y)	u(x)	u(x)	u(x)	u(x)	u(x)	u(x)
332.65	4E-05	2E-03	6E-05	7E-05	5E-05	2E-05	2E-04	5E-04	4E-05	2E-03
364.56	6E-05	2E-03	2E-04	2E-04	4E-05	2E-05	2E-04	4E-04	6E-05	2E-03

[a] Expanded uncertainties (k=2) U(P)=0.0008MPa, U(T)=0.02K [b]Vapor water content is not measured and lower than the limit of detection of the TCD detector

Table 20: Partition coefficient of Ethanethiol (1839) in 25 wt% MDEA aqueous solution with CO_2 and H_2S (respective total loadings 0.234 and 0.200). δx corresponds to the standard deviation due to repeatability measurements and u(x) corresponds to uncertainties due to GC detectors calibration.

T[a]	P[a]		EM		CH_4		CO_2		H_2S		MDEA		H_2O[b]		Loadings	
K	MPa	n	x	δx	x	δx	x	δx	x	δx	x	δx	x	δx	CO_2	H_2S
333.73	7.0165	6	0.00062	5E-06	0.00153	3E-06	0.01021	6E-05	0.00804	8E-05	0.04700	4E-06	0.93259	7E-05	0.217	0.171
365.58	6.9835	5	0.00056	2E-06	0.00162	3E-06	0.00840	5E-05	0.00748	6E-05	0.04712	3E-06	0.93483	6E-05	0.178	0.159

T[a]	P[a]		EM		CH_4		CO_2		H_2S	
K	MPa	n	y	δy	y	δy	y	δy	y	δy
333.73	7.0165	6	0.00629	2E-04	0.98931	2E-04	0.00313	8E-05	0.00127	2E-05
365.58	6.9835	5	0.00738	7E-05	0.97643	2E-04	0.01241	7E-05	0.00379	7E-05

T	EM	CH_4	CO_2	H_2S	EM	CH_4	CO_2	H_2S	MDEA	H_2O
K	u(y)	u(y)	u(y)	u(y)	u(x)	u(x)	u(x)	u(x)	u(x)	u(x)
333.73	4E-05	4E-03	2E-05	3E-05	2E-05	2E-05	1E-04	2E-04	4E-05	4E-03
365.58	4E-05	4E-03	7E-05	9E-05	2E-05	2E-05	1E-04	2E-04	4E-05	4E-03

[a] Expanded uncertainties (k=2) U(P)=0.0008MPa, U(T)=0.02K [b]Vapor water content is not measured and lower than the limit of detection of the TCD detector

Table 21: Partition coefficient of Ethanethiol in 25 wt% MDEA aqueous solution with CO_2 and H_2S (respective total loadings 0.234 and 0.413) (global concentration of EM: 1839 ppm). δx corresponds to the standard deviation due to repeatability measurements and u(x) corresponds to uncertainties due to GC detectors calibration.

T[a]	P[a]		EM		CH_4		CO_2		H_2S		MDEA		H_2O[b]		Loadings	
K	MPa	n	x	δx	x	δx	x	δx	x	δx	x	δx	x	δx	CO_2	H_2S
333.75	7.0290	6	0.00068	6E-06	0.00151	2E-06	0.00945	3E-05	0.01815	8E-05	0.04655	4E-06	0.92365	8E-05	0.203	0.390
365.58	7.0118	7	0.00056	6E-06	0.00158	4E-06	0.00730	5E-05	0.01665	2E-04	0.04673	8E-06	0.92718	2E-04	0.156	0.356

T[a]	P[a]		EM		CH_4		CO_2		H_2S	
K	MPa	n	y	δy	y	δy	y	δy	y	δy
333.75	7.0290	5	0.00576	6E-05	0.98498	1E-04	0.00455	7E-05	0.00471	8E-05
365.58	7.0118	10	0.00795	1E-04	0.96419	3E-04	0.01604	2E-04	0.01181	2E-04

T	EM	CH_4	CO_2	H_2S	EM	CH_4	CO_2	H_2S	MDEA	H_2O
K	u(y)	u(y)	u(y)	u(y)	u(x)	u(x)	u(x)	u(x)	u(x)	u(x)
333.75	3E-05	4E-03	2E-05	1E-04	2E-05	2E-05	1E-04	5E-04	3E-05	4E-03
365.58	5E-05	4E-03	8E-05	3E-04	2E-05	2E-05	1E-04	4E-04	5E-05	4E-03

[a] Expanded uncertainties (k=2) U(P)=0.0008MPa, U(T)=0.02K [b]Vapor water content is not measured and lower than the limit of detection of the TCD detector

Table 22: Partition coefficient of Ethanethiol (1839 ppm) in 25 wt% MDEA aqueous solution with CO_2 and H_2S (respective total loadings 0.404 and 0.202). δx corresponds to the standard deviation due to repeatability measurements and u(x) corresponds to uncertainties due to GC detectors calibration.

T[a]	P[a]		EM		CH_4		CO_2		H_2S		MDEA		H_2O[b]		Loadings	
K	MPa	n	x	δx	x	δx	x	δx	x	δx	x	δx	x	δx	CO_2	H_2S
333.77	6.6937	7	0.00064	7E-06	0.00152	7E-06	0.01850	7E-05	0.00839	6E-05	0.04659	5E-06	0.92436	1E-04	0.397	0.180
365.60	7.0410	8	0.00056	3E-06	0.00161	3E-06	0.01445	5E-05	0.00773	9E-05	0.04681	3E-06	0.92884	6E-05	0.309	0.165

T[a]	P[a]		EM		CH_4		CO_2		H_2S	
K	MPa	n	y	δy	y	δy	y	δy	y	δy
333.77	6.6937	5	0.00610	6E-05	0.98297	8E-05	0.00851	5E-05	0.00243	1E-05
365.60	7.0410	5	0.00810	9E-05	0.95725	1E-04	0.02920	2E-05	0.00544	1E-04

T	EM	CH_4	CO_2	H_2S	EM	CH_4	CO_2	H_2S	MDEA	H_2O
K	u(y)	u(y)	u(y)	u(y)	u(x)	u(x)	u(x)	u(x)	u(x)	u(x)
333.77	4E-05	4E-03	5E-05	6E-05	2E-05	2E-05	3E-04	2E-04	4E-05	4E-03
365.60	5E-05	4E-03	2E-04	1E-04	2E-05	2E-05	2E-04	2E-04	5E-05	4E-03

[a] Expanded uncertainties (k=2) U(P)=0.0008MPa, U(T)=0.02K [b]Vapor water content is not measured and lower than the limit of detection of the TCD detector

Table 23: Methanethiol and Ethanethiol partition coefficient and apparent Henry's Law constant in 25 wt% MDEA aqueous solution at 333 and 363 K.

Methanethiol (2438 ppm)			Ethanethiol (2281 ppm)		
P_{total}/MPa	K_{MM}	H_{MM}/MPa	P_{total}/MPa	K_{EM}	H_{EM}/MPa
333 K					
Gas stripping method		6.1	**Gas stripping method**		15.0
2.0033	16.31	32.7	2.1754	14.6	31.9
4.0292	9.45	38.1	4.0419	9.4	38.0
7.0543	6.08	42.9	6.9601	7.2	50.5
365 K					
Gas stripping method		14.5	**Gas stripping method**		39.1
1.9405	28.89	56.1	2.0088	26.7	53.6
4.0580	15.40	62.4	4.0410	15.6	63.1
7.0408	9.58	67.5	7.1768	11.7	84.0

In order to characterise the dependency of the apparent Henry's law constant to the concentration of mercaptan, we have modified our experimental procedure. Tests were only done with ethanethiol. We did not introduced ethanethiol directly in the vessel with the solvent. We have injected a known quantity of ethanethiol using a GC syringe directly in the equilibrium cell. Solvent, composed with only water and MDEA, is after introduced into the equilibrium cell. We have measured the concentration of each phase and determined the apparent Henry's law constant. We have realized the measurement considering seven injections in order to have a global concentration of ethanethiol (EM) comprise between 200 and 1199 ppm. Results are presented on figure 5. Our results seem to confirm that apparent Henry's law constant depends on the global ethanethiol concentration. Moreover, we can also observe on figure 5 that we have a lot of dispersion. This can be attributed to the fact the injection is not so accurate. These tests have validated our choice to introduce the mercaptan directly in the MDEA solution and not separately.

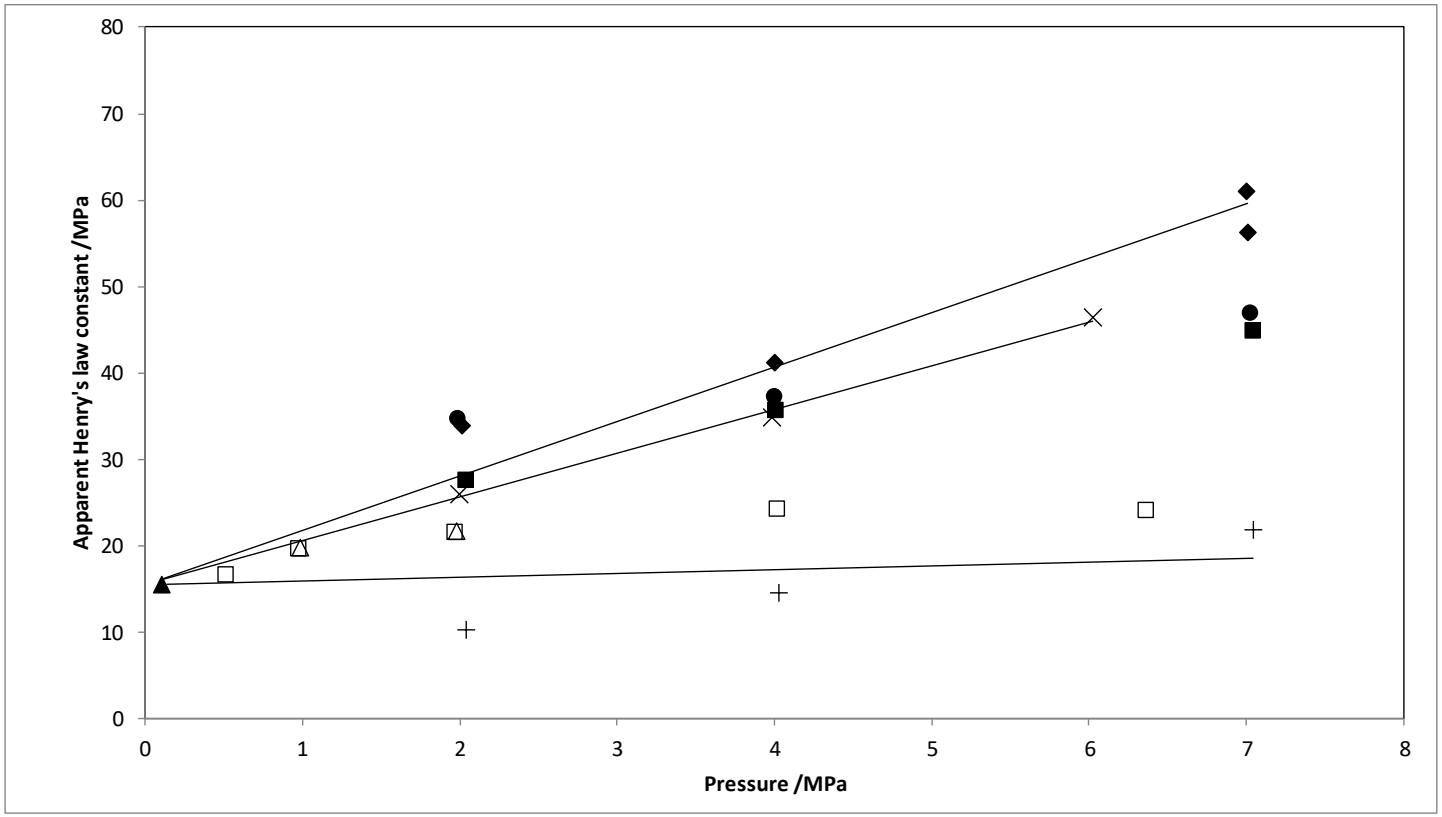

Figure 5: Variation of ethanethiol (EM) apparent Henry's law constant in 25 wt% MDEA aqueous solution as a function of total pressure for various EM concentrations. Δ: 200ppm, ×: 998 ppm, +: 398 ppm, □: 401 ppm, ♦: 2000 ppm, ●: 1199 ppm, ■: 690 ppm, ▲: gas stripping method (exponential dilutor).

2.4. Discussions

According to Table 23, we can observed that the apparent Henry's law constant increase with the addition of CH_4 (increasing of total pressure). According to the Tables 24 to 26, we can observed that the apparent Henry's law constant increase with the addition of acid gases (CO_2, H_2S and CO_2+H_2S). Also, results with pure CO_2 and pure H_2S are plotted on figures 6 and 7 respectively. This can be attributed by a drop out phenomenon: CO_2 and H_2S are better solubilized than mercaptan due to their strongest acid base reaction. Consequently, electrolytes are produced and lead to a salting out effect for the mercaptans and so concentration of mercaptan decreases in the liquid phase and increases in the vapour phase. We can also observed that this effect is more pronounced with CO_2 and for ethanethiol. With CO_2 we have creation of bicarbonate ($R_2NHCH_3HCO_3$) which are ions with a more important size and so have a more important contribution to the entropy of the aqueous solution (higher activity coefficient). Solubility of MM is higher than the solubility of EM. It is due to the fact that ethanethiol have 2 carbon atoms (solvation effect with MM needs less molecule of water). Figures 6 and 7 shows the variation of the apparent Henry's law constant with acid gas loading.

Table 24: Methanethiol and ethanethiol partition coefficient and apparent Henry's Law constant in 25 wt% MDEA aqueous solution at 333 and 363 K and around 7 MPa in the presence of CO_2.

Methanethiol (2438 ppm)			Ethanethiol (2281 ppm)		
CO_2 loading	K_{MM}	H_{MM}/MPa	CO_2 loading	K_{EM}	H_{EM}/MPa
			333 K		
0	-	49.6	0		50.5
0.187	10.07	70.5	0.155	12.93	90.6
0.481	12.09	84.5	0.309	15.52	109.2
			365 K		
0	-	78.5	0		84.0
0.229	14.60	102.3	0.140	17.23	120.7
0.413	15.52	108.8	0.253	19.56	136.6

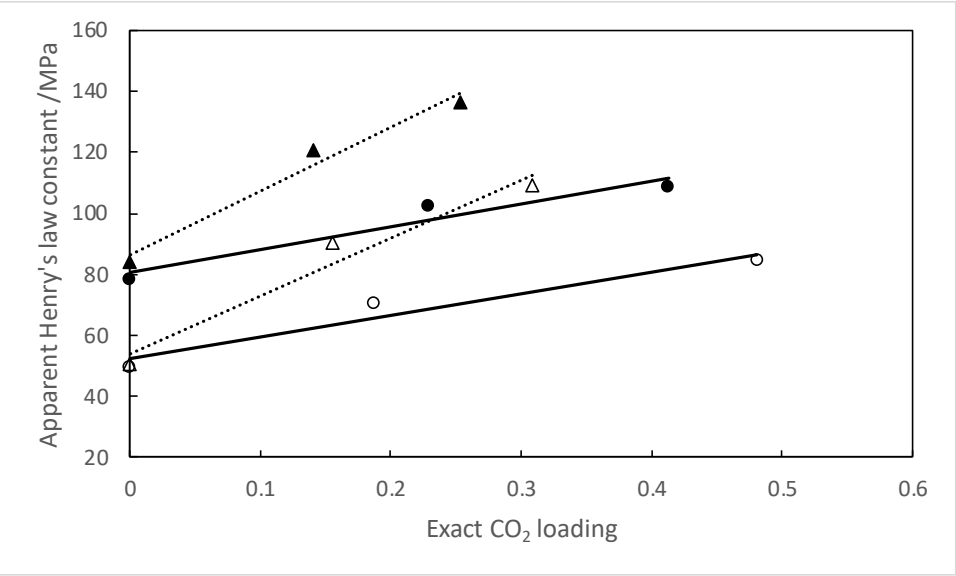

Figure 6: Variation for Methanethiol (o) and Ethanethiol (Δ) apparent Henry's law constant as a function CO_2 loading. Empty symbol: 333K, black symbol: 365 K. Lines: linear tendency curve.

Table 25: Methanethiol and ethanethiol partition coefficient and apparent Henry's Law constant in 25 wt% MDEA aqueous solution at 333 and 363 K and around 7 MPa in the presence of H_2S.

Methanethiol (2438 ppm)			Ethanethiol (2281 ppm)		
H_2S loading	K_{MM}	H_{MM}/MPa	H_2S loading	K_{EM}	H_{EM}/MPa
			333 K		
0		49.6	0	-	50.5
0.206	8.74	61.2	0.132	9.98	69.7
0.368	9.03	63.1	0.320	11.08	77.4
			365 K		
0		78.5	0	-	84.0
0.192	11.68	82.7	0.101	13.34	93.5
0.344	13.57	94.6	0.307	15.18	106.0

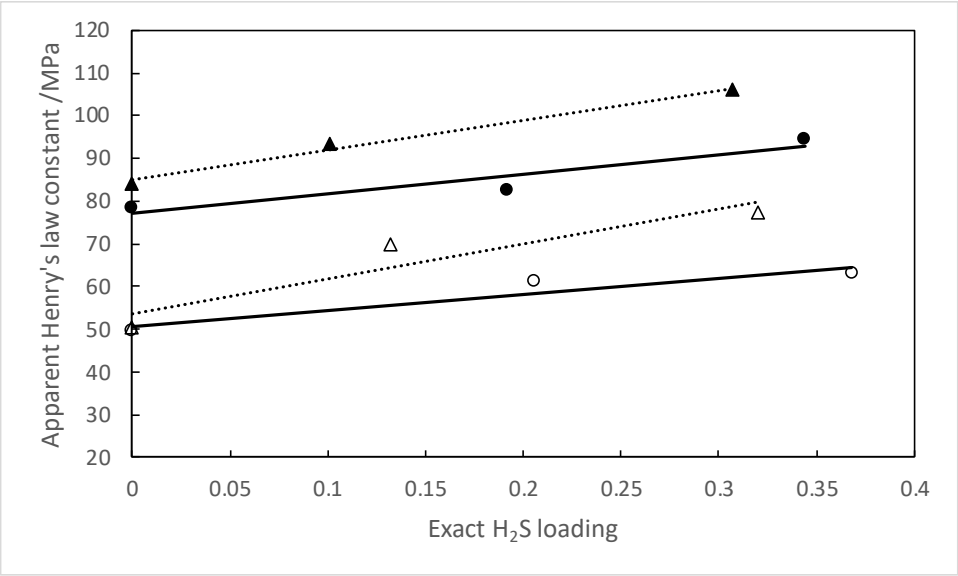

Figure 7: Variation for Methanethiol (o) and Ethanethiol (Δ) apparent Henry's law constant as a function H_2S loading. Empty symbol: 333K, black symbol: 365 K. Lines: linear tendency curve.

Table 26: Methanethiol and ethanethiol partition coefficient and apparent Henry's Law constant in 25 wt% MDEA aqueous solution at 333 and 363 K and around 7 MPa in the presence of H_2S.

Methanethiol (2438 ppm)				Ethanethiol (2281 ppm)			
CO_2 loading	H_2S loading	K_{MM}	H_{MM}/MPa	CO_2 loading	H_2S loading	K_{EM}	H_{EM}/MPa
333 K							
0	0	-	49.6	0	0	-	50.5
0.252	0.224	8.71	60.9	0.217	0.171	10.20	71.6
0.428	0.235	7.68	53.6	0.203	0.390	8.46	59.7
0.197	0.448	7.23	50.1	0.397	0.180	9.55	63.9
365 K							
0	0	-	78.5	0	0	-	84.0
0.209	0.212	12.91	89.8	0.178	0.159	13.05	91.2
0.300	0.199	13.15	92.7	0.156	0.356	14.09	98.8
0.165	0.395	11.30	75.7	0.309	0.165	14.47	101.9

From Table 26, it is possible to observe the influence of the two acid gases on apparent Henry's law constant. In Figure 8, we have plotted the variation of apparent Henry's law constant of the two mercaptans as a function of CO_2 loading but for an approximate given loading of H_2S equal to 0.2 for methanethiol and 0.17-0.16 for ethanethiol. As we can observed, H_2S reduces the slope of apparent Henry's law constant versus the CO_2 loading curve. The concentration of mercaptan in the liquid phase decreases but in parallel, as we have introduced also some H_2S, the vapor concentration decreases more strongly.

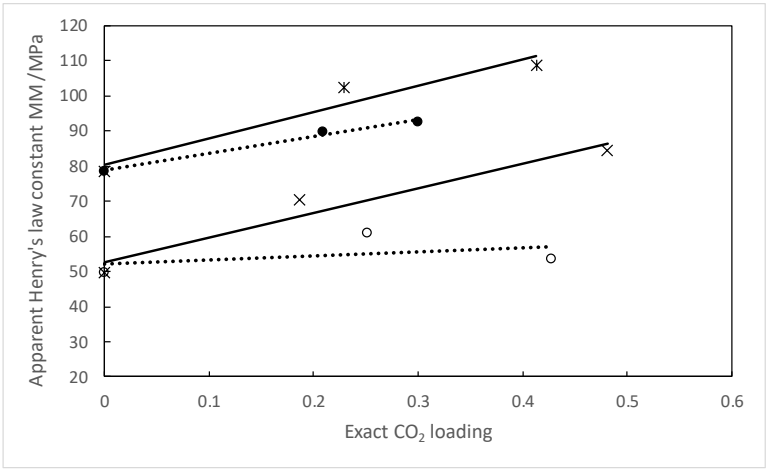

A

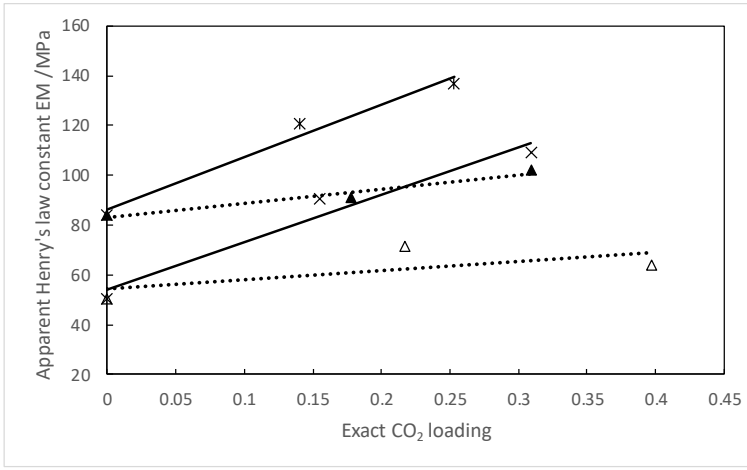

B

Figure 8: Variation of Methanethiol (o, A) and Ethanethiol (Δ, B) apparent Henry's law constant as a function CO_2 loading (H_2S loading is fixed). Empty symbol: 333K, black symbol: 365 K. Lines: linear tendency curve. ×: without H_2S at 333K, *: with H_2S at 365 K.

The last point to be analyzed is the impact of CO_2 and H_2S separately on mercaptan solubility. We have considered the ratios $x_{MM}/x_{MM,without\ acid\ gas}$ and $x_{EM}/x_{EM,without\ acid\ gas}$. It is another way to observe the drop out effects due to addition of acid gases. The ratios are equal to one without acid gas. Figures 9 and 10 show the influence of acid gas loading (CO_2 and H_2S) for ethanethiol and methanethiol ratios for each temperature respectively. We can see that with CO_2 the ratio decreases strongly. With H_2S, the ratio seems to increase before decreasing. Moreover, we can also observed that methanethiol does not behave like ethanethiol. With methanethiol, addition of acid gas seems to increase its solubility in comparison to its solubility in the solution without acid gas before decreasing. This effect is more pronounced with H_2S. Can we consider that with H_2S, the interaction between methanethiol and the solvent is stronger in comparison to the one between ethanethiol and the solvent (size effect, chemical reaction, etc..)? And consequently, leading to a higher solubility? It seems that it happens also with CO_2 at low temperature. We can say that it may exists a weakly reactive chemical reaction between with methanethiol (MM) and MDEA. To conclude this study, we propose to summarize in figure 11 the thermodynamic behaviour of mercaptan considering the apparent Henry's law constant as a function of total pressure (due to introduction of methane) and acid gases loading (CO_2 and/or H_2S). Starting of apparent Henry's law constant without methane and acid gas (for example, obtained by gas stripping method), we can say that apparent Henry's law constant increases with pressure and addition of acid gases. It also increases if we increase the global concentration of mercaptan.

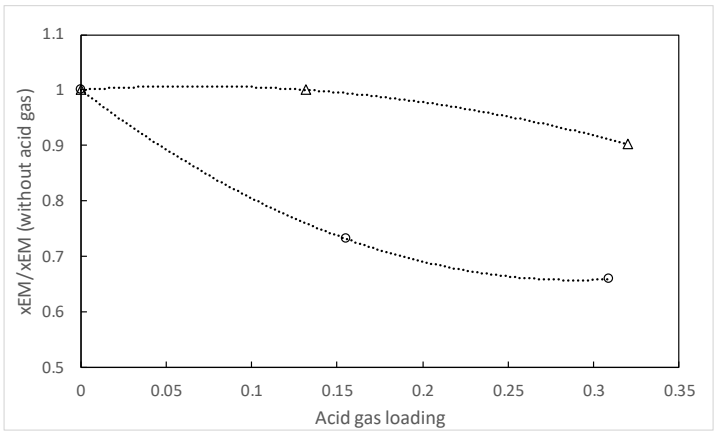

A

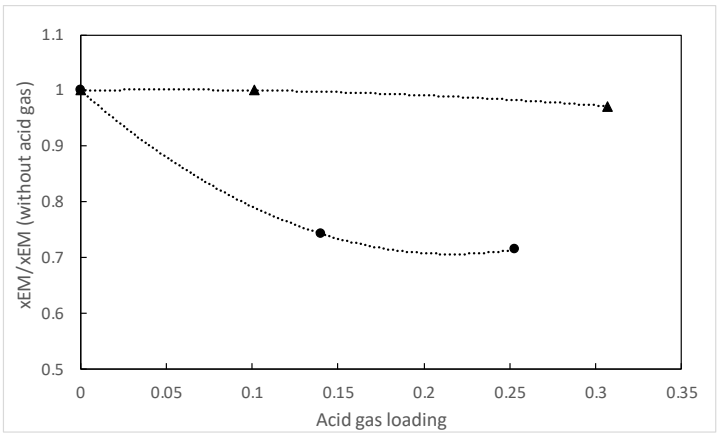

B

Figure 9: Influence of H_2S (Δ) and CO_2 (o) on the solubility of ethanethiol (EM) in 25wt% MDEA aqueous solution (A: 333K, B: 365K) at pressure around 7 MPa.

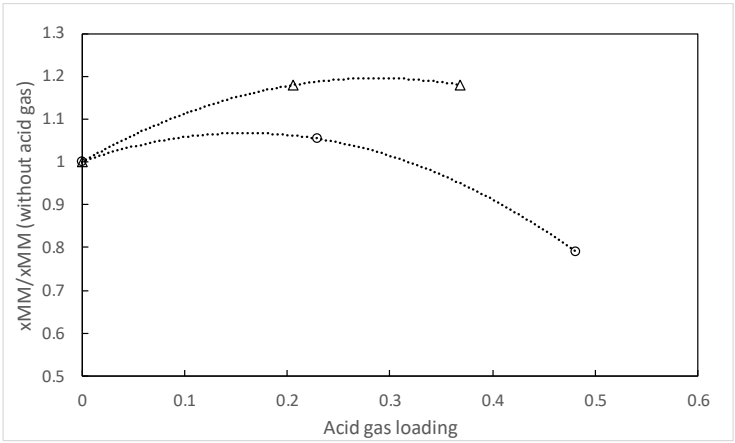

A

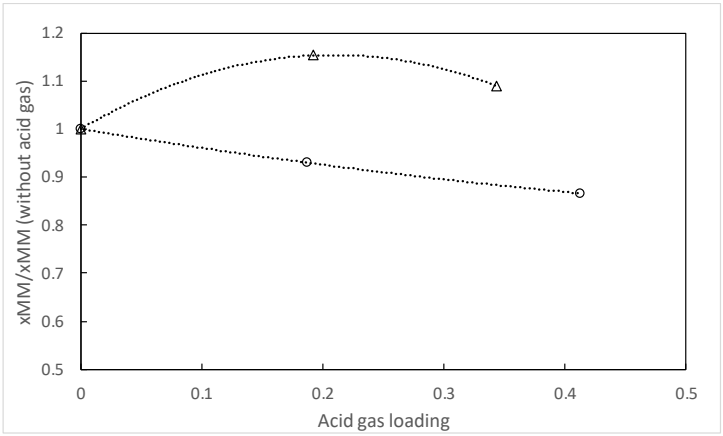

B

Figure 10: Influence of H_2S (Δ) and CO_2 (o) on the solubility of methanethiol (MM) in 25wt% MDEA aqueous solution (A: 333K, B: 365K).

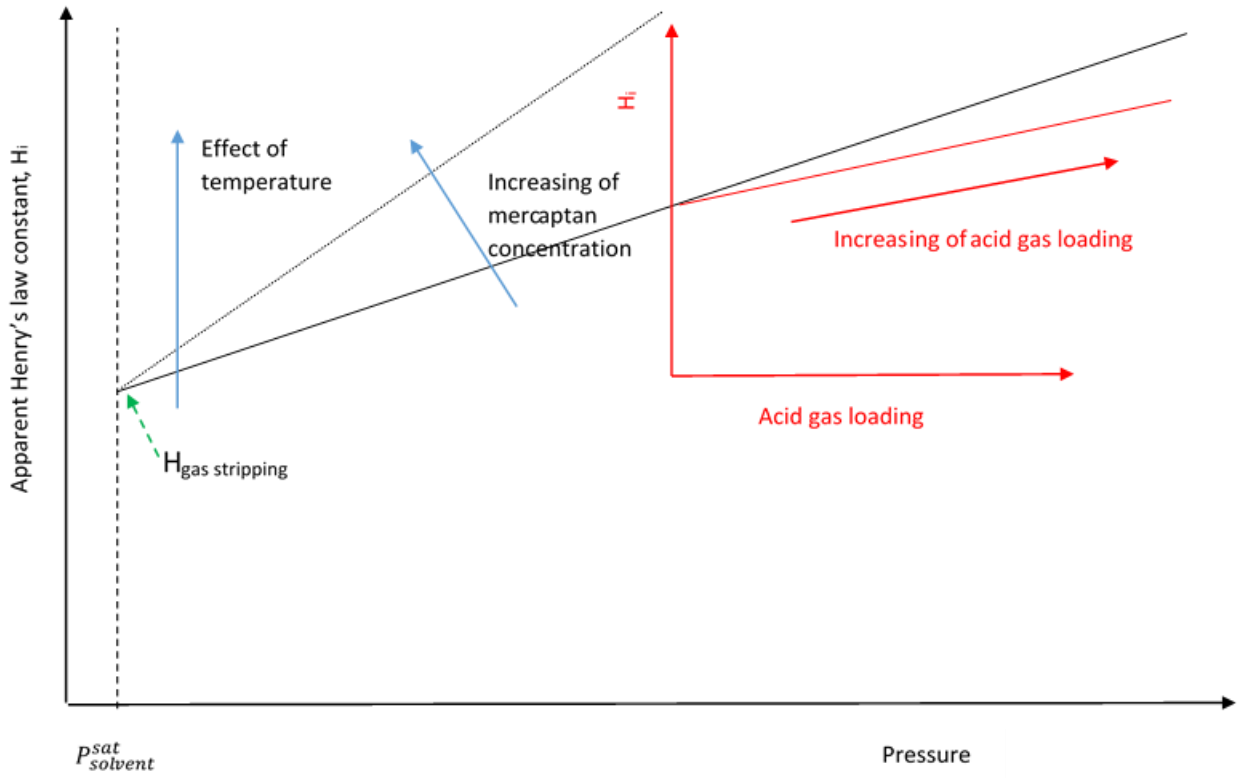

Figure 11: Apparent Henry's law constant of mercaptan as a function of global mercaptan concentration, total pressure and acid gas loading.

We have analysed the results obtained by Jou and Mather[10] considering our method of analysis. In figure 12, we have plotted the apparent Henry's law constant as a function of CO_2 and H_2S loadings. We remind that Jou and Mather have done their measurements at constant total pressure 6.89 MPa. We observe the same tendency with their data like with ours. The slight dispersion maybe due to the fact that the global methanethiol concentration is not the same for all the measurements done by Jou and Mather. Moreover, using their data we can also show that the apparent Henry's law constant increase when the concentration of methanethiol increases.

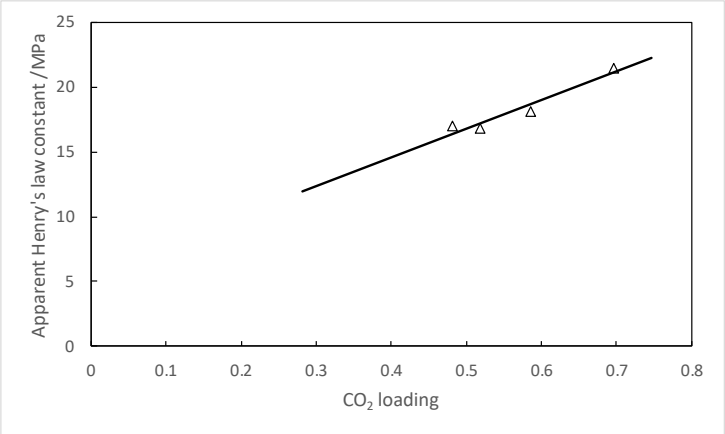

A

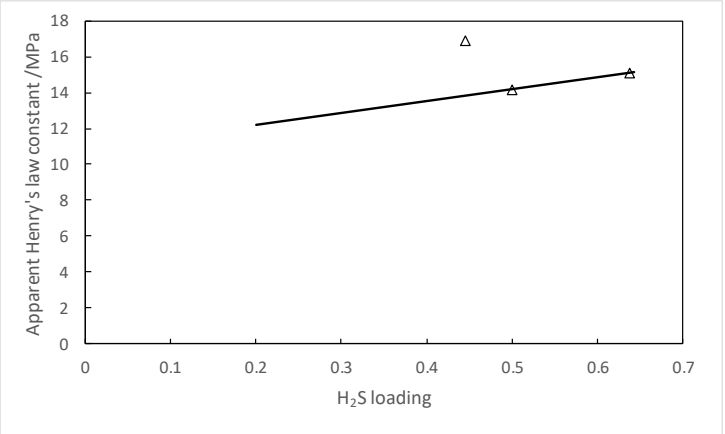

B

Figure 12: Variation of MM (Δ) apparent Henry's law constant as a function CO_2 loading (A) and H_2S loading (B) at 40°C form data form Jou and Mather[9].

CONCLUSION

We have obtained new experimental data concerning the partition coefficient of methanethiol and ethanethiol in 25wt% aqueous MDEA solution in the presence or not of acid gases. Two different techniques were used. The exponential dilutor (gas stripping method) was used to determine the apparent Henry's law constant at the vapour pressure of the solvent and an equipment based on "static analytic method" with two capillary samplers connected to gas chromatograph was used to determine the concentrations of the vapour and liquid phases, particularly the concentrations of methanethiol and ethanethiol in each phase. The solubility of ethanethiol decreases after introduction of acid gases and consequently, the apparent Henry's constant becomes larger. With methanethiol we observe an increasing and a decreasing of solubility after addition of acid gases and an increasing of apparent Henry's law constant. Increasing of temperature leads to decrease the mercaptan solubility and to increase the apparent Henry's law constant.

Acknowledgements

The authors are grateful to the Gas Processors Association (GPA Midstream) for the financial support of this work.

REFERENCES

[1] Bedell, S.A.; Miller, M., Aqueous amines as reactive solvents for mercaptan removal. *Ind. Eng. Chem. Res*. **2007**, 46, 3729-3733

[2] K. Osman, K.; Coquelet, C.; Ramjugernath, D. Review of carbon dioxide capture and storage with relevance to South African power sector. *South Africa J. Sc.* **2014**, 110, 1-12

[3] Huguet, E. ; Coq, B. ; Durand, R. ; Leroi, C. ; Cadours, R. ; Hulea, V. A highly efficient process for transforming methylmercaptan into hydrocarbons and HS on solid acid catalysts *Applied Catalysis B*. **2013**, 134– 135, 344-348

[4] Awan, J. A.; Kontogeorgis, G. M.; Tsivintzelis, I.; Coquelet, C. Vapor–liquid–liquid equilibrium measurements and modeling of ethanethiol+ methane+ water, 1-propanethiol+ methane+ water and 1-butanethiol+ methane+ water ternary systems at 303, 335, and 365 K and pressure up to 9 MPa. *Ind. Eng. Chem. Res.* **2013,** *52*(41), 14698-14705.

[5] Pellegrini, L.A. ; Langè, S ; Moioli, S.;Picutti, B. ; Vergani,P. Influence of gas impurities on thermodynamics of amine solutions. 1. Aromatics. *Ind. Eng. Chem. Res*. **2013**, 52, 2018-2024.

[6] Langè, S. ; Pellegrini, L.A. ; Moioli, S.; Picutti, B. ; Vergani, P Influence of gas impurities on thermodynamics of amine solutions. 2. Mercaptans. *Ind. Eng. Chem. Res.* **2013**, 52, 2025–2031

[7] Awan, J.A.; Valtz,, A. Coquelet, C.; Richon, D. Effect of acid gases on the solubility of n-propylmercaptan in 50wt% methyl-diethanolamine aqueous solution, *Chem. Eng. Research and. Design*. **2008**, 86, 600-605.

[8] Coquelet, C.; Richon, D. Measurement of Henry's law constants and infinite dilution activity coefficients of propyl mercaptan, butyl mercaptan and dimethyl sulfide in water and in 50 wt % methyldiethanolamine aqueous solution using a gas stripping technique, *J. Chem. Eng. Data* **2005**, 50, 2053-2057.

[9] Coquelet, C.; Laurens, S.; Richon, D. Measurement of Henry's law constants and infinite dilution activity coefficients of Propyl Mercaptan, Butyl Mercaptan and Dimethyl Sulfide in water and in 25, 35 and 50 wt % Methyldiethanolamine aqueous solutions using a gas stripping technique, *J. Chem. Eng. Data* **2008**, 53, 2540-2543.

[10] Jou, F. Y.; Mather, A. E.; Ng, H. J. Effect of CO_2 and H_2S on the Solubility of Methanethiol in an Aqueous Methyldiethanolamine Solution. *Fluid Phase Equilib.* **1999**, *158*, 933-938.

[11] Zin, R.M.; Coquelet, C.; Valtz, A.; Mutalib, M.I.A.; Sabil, K.M. Measurement of Henry's Law Constant and Infinite Dilution Activity Coefficient of Isopropyl Mercaptan and Isobutyl Mercaptan in Methyldiethanolamine (1)+ Water (2) with w 1= 0.25 and 0.50 at temperature of 298 to 348K using Inert Gas Stripping Method. *J. Chem. Therm*. **2016**, 93, 193-199

[12] Hajiw, M.; Valtz, A.; El-Ahmar, E.; Coquelet, C. How measurement of limiting activity coefficient can help for the selection of solvents for oxygenated compounds extraction. *J. Env. Chem. Eng.* **2017**, 5, 1205-1209.

[13] Kim, I., Svendsen, H.F., Borresen, E. Ebulliometric determination of vapour-liquid Equilibria for pure water, monoethanolamine, N-methyldiethanolamine, 3-(methylamino)-propylamine, and their binary and ternary solutions. *J. Chem. Eng. Data* **2008**, 53, 2521-2531.

[14] Dicko, M.; Coquelet, C.; Jarne, C.; Northrop, S.; Richon, D. Acid Gases Partial Pressures above a 50 wt% aqueous Methyldiethanolamine Solution. Experimental work and modeling, *Fluid Phase Equilib.* **2010**, 289, 99-109

[15] E Skylogianni, E.; Mundal, I.; Pinto, D.; Coquelet, C.; Knuutila, H.K. Hydrogen sulfide solubility in 50 wt% and 70 wt% aqueous methyldiethanolamine at temperatures from 283 to 393 K and total pressures from 500 to 10000 kPa. *Fluid Phase Equilib.* **2020**, 112498

[16] Lemmon, E.; Bell, I. H.; Huber, M.; McLinden, M., NIST Standard Reference Database 23: Reference Fluid Thermodynamic and Transport Properties-REFPROP, Version 10.0, National Institute of Standards and Technology. **2018**. *URL http://www.nist. gov/srd/nist23. cfm*.

[17] Zin, R.M.; Coquelet, C.; Valtz, A.; Mutalib, M.I.A.; Sabil, K.M. A New Thermodynamic Correlation for Apparent Henry's Law Constants, Infinite Dilution Activity Coefficient and Solubility of Mercaptans in Pure Water. *J. Natural Gas Eng.* **2017**, 2, 148-170

[18] Gas Processors Suppliers Association, GPSA, 2018, *Engineering Data Book*, 14th Edition, Tulsa, OK.

[19] Chapoy, A.; Coquelet, C.; Richon, D. Solubility measurement and modeling of water in the gas phase of the methane/water binary system at temperatures from 283.08 to 318.12 K and pressures up to 34.5 MPa. *Fluid Phase Equilib.* **2003**, 214, 101-117.

[20] Chapoy, A.; Coquelet, C.;Richon, D. Corrigendum to "Revised solubility data and modeling of water in the gas phase of the methane/water binary system at temperatures from 283.08 to 318.12 K and pressures up to 34.5 MPa". *Fluid Phase Equilib.* **2005**, 230, 210-214.

TOC Graphic

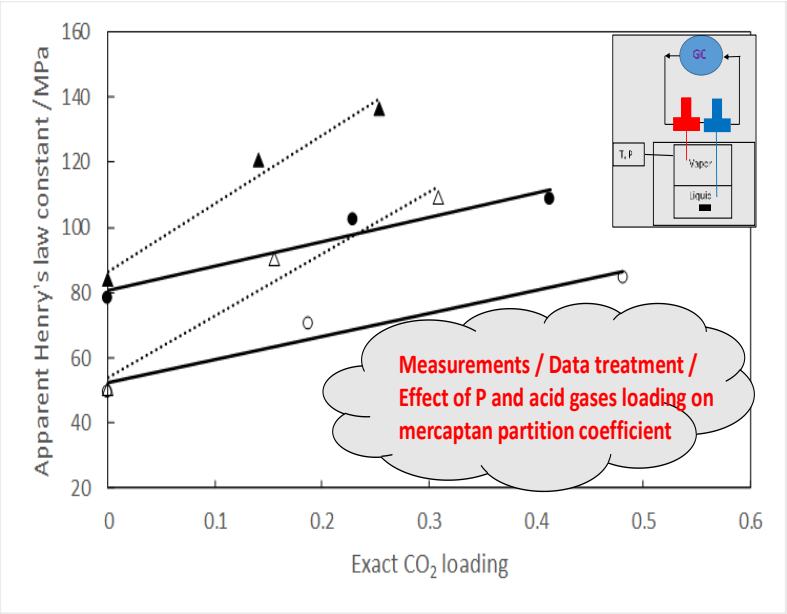
Apparent Henry's law constant /MPa
160
140
120
100
80
60
40
20
0
0.1
0.2
0.3
0.4
0.5
0.6
Exact CO_2 loading
GC
T, P
Vapor
Liquid
Measurements / Data treatment /
Effect of P and acid gases loading on
mercaptan partition coefficient